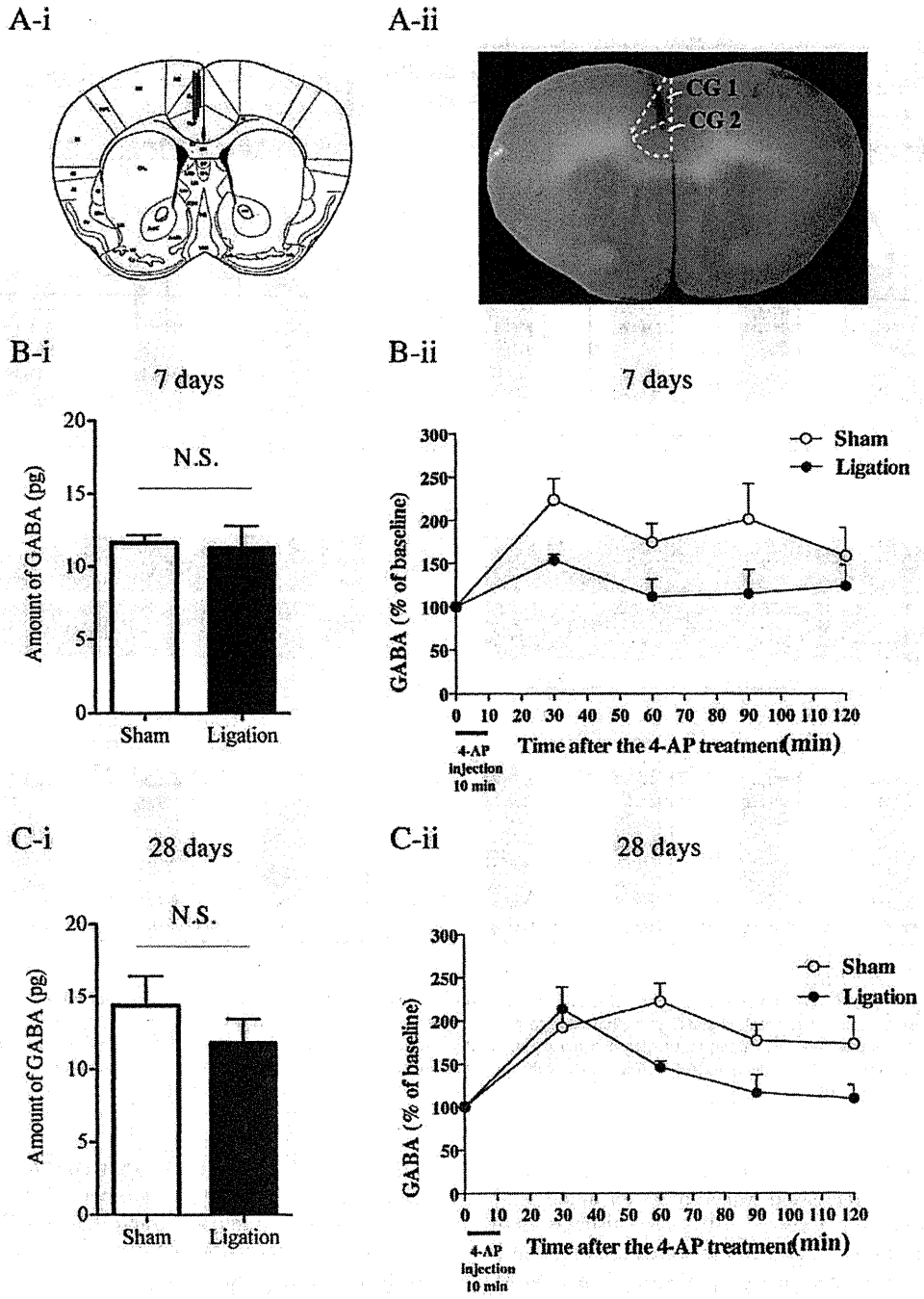

Fig. 6. Changes in 4-aminopyridine (4-AP)-induced extracellular GABA release under a neuropathic pain-like state. Schematic reconstruction of microdialysis probe (vertical bars) placements within the cingulate cortex was shown in (A-i). Length of vertical bars corresponds to the length of the active portion of the dialysis membrane (1.0 mm). Photomicrograph showed a vestige of microdialysis probe. Blue-ink was microinjected into the same position as microdialysis probe after the experiment (A-ii). There were no changes in the basal level of GABA in sham-operated and sciatic nerve-ligated mice at 7 days (B-i) or 28 days (C-i) after surgery (N.S.; not significant). Effects of treatment with 4-AP on the extracellular level of GABA in the cingulate cortex of sham-operated and sciatic nerve-ligated mice at 7 days (B-ii) or 28 days (C-ii) after surgery. 4-AP (1 mM) was injected into the cingulate cortex for 10 min. GABA release in the cingulate cortex was significantly decreased in nerve-ligated mice at 7 days after surgery. Two-way ANOVA was performed, followed by Bonferroni testing. Each point represents the mean ± SEM of 6 to 8 mice.

mice, indicating that neuropathic pain-like stimuli may predominantly promote the long-lasting membrane translocation of GAT-3 in the frontal cortex. In the present double-staining approach, we found that GAT-3 IR in the cingulate cortex of nerve-ligated mice was clearly co-localized with activated GFAP-positive astrocytes, which is supported by the finding that GAT-3 is mainly located on astrocytes [54]. These findings support the idea that neuropathic pain may increase GABA reuptake via increased membrane-bound GAT-3 in activated astrocytes of the cingulate cortex.

To clarify whether the extracellular level of GABA in the cingulate cortex could be altered under a long-lasting pain-like state, an in vivo microdialysis study was performed. The GABA level at the synaptic cleft in the cingulate cortex was significantly decreased in nerve-ligated mice after the administration of 4-AP. These results suggest that neuropathic pain can decrease endogenously released GABA at the synaptic cleft associated with an increase in the reuptake of GABA via increased GAT-3 located on activated astrocytes, which diminishes the efficiency of GABAergic neurotransmission in the cingulate cortex.

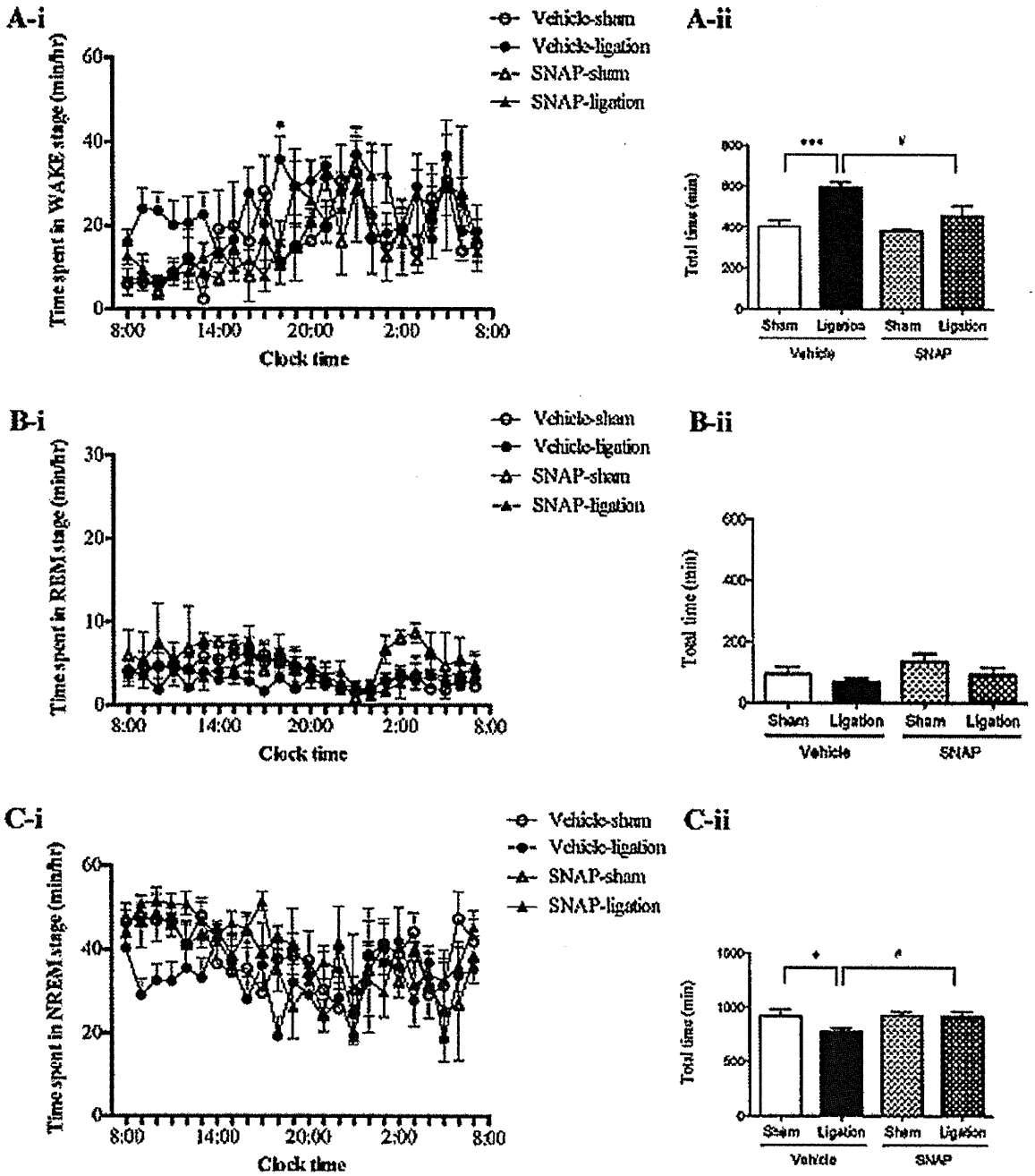

Fig. 7. Changes in sleep vigilance after the intracingulate cortex injection of SNAP-5114 under a neuropathic pain-like state as determined by EEG/EMG recordings. Sleep–wake states after the microinjection of vehicle or SNAP-5114 into the cingulate cortex at 7 days after sciatic nerve ligation. Vehicle or SNAP-5114 (1 nmol/mouse) was injected at 8:00 AM. Time spent in the WAKE stage (A-i, ii), REM sleep stage (B-i, ii) and NREM sleep stage (C-i, ii) was determined by EEG/EMG recording. The increased WAKE stage (A-ii) and decreased NREM stage (C-ii) were significantly attenuated by the intracingulate cortex injection of SNAP-5114 in nerve-ligated mice compared to those in sham-operated mice (A-i, B-i, and C-i). The statistical analysis was performed by 2-way ANOVA and the Bonferroni test (unless otherwise indicated). (A-ii, B-ii, and C-ii) The statistical analysis was performed by Student's *t*-test. Each bar represents the mean ± SEM of 5 to 6 mice. $^{*}P < .05$ and $^{***}P < .001$ vs sham group, $^{\#}P < .05$ vs ligation group.

In the present EEG/EMG analysis, we found that the increased WAKE stage and decreased NREM stage under a neuropathic pain-like state were almost reset by microinjection of the GAT-3 inhibitor SNAP-5114 into the cingulate cortex. These findings indicate that the increase in membrane-translocated GAT-3 on activated astrocytes, which can uptake and metabolize GABA released at the synaptic cleft, in the cingulate cortex area may be accompanied by sleep disturbance under a neuropathic pain-like state.

In general, it has been considered that excitatory and inhibitory transmission maintain a physiological balance in the normal state. A recent study by Xu et al. [61] suggests that both presynaptic and postsynaptic excitatory glutamatergic transmission are enhanced in the anterior cingulate cortex of mice with neuropathic pain. Although further experiments are still needed, these phenomena may explain the loss of the balance between excitatory and inhibitory transmission in the cingulate cortex under neuropathic pain.

It has been established that benzodiazepines decrease wakefulness through the enhanced affinity of endogenous GABA binding to $GABA_A$ receptors [2,20]. Considerable evidence indicates that benzodiazepines, such as midazolam and zolpidem, cannot independently elicit the influx of Cl^- ions through the $GABA_A$ receptor,

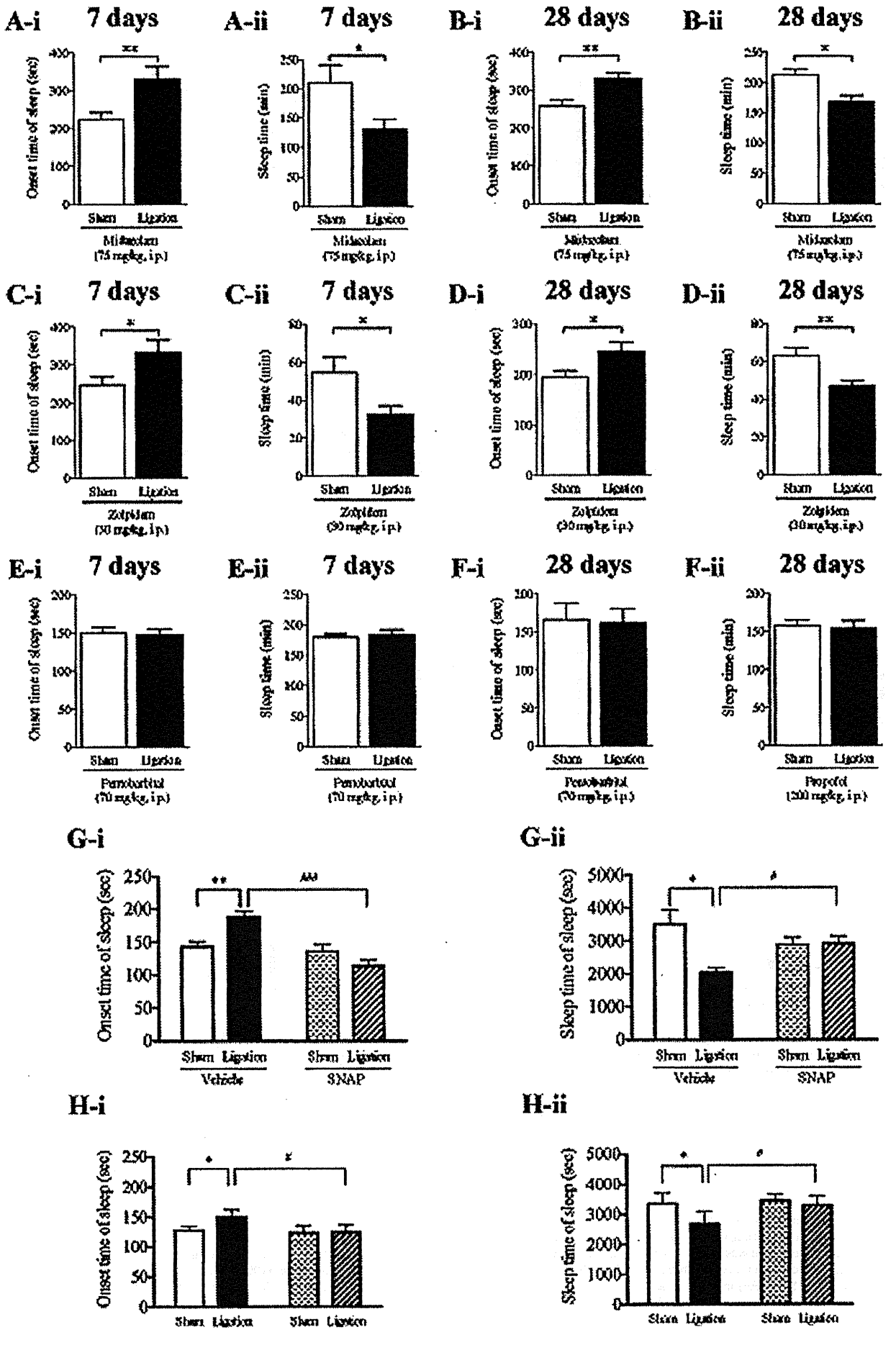
A-i
7 days
A-ii
7 days
B-i
28 days
B-ii
28 days
C-i
7 days
C-ii
7 days
D-i
28 days
D-ii
28 days
E-i
7 days
E-ii
7 days
F-i
28 days
F-ii
28 days
Onset time of sleep (sec)
Sleep time (min)
Sham
Ligation
Midazolam
(75 mg/kg, i.p.)
Zolpidem
(30 mg/kg, i.p.)
Pentobarbital
(70 mg/kg, i.p.)
Propofol
(200 mg/kg, i.p.)
G-i
G-ii
H-i
H-ii
Vehicle
SNAP

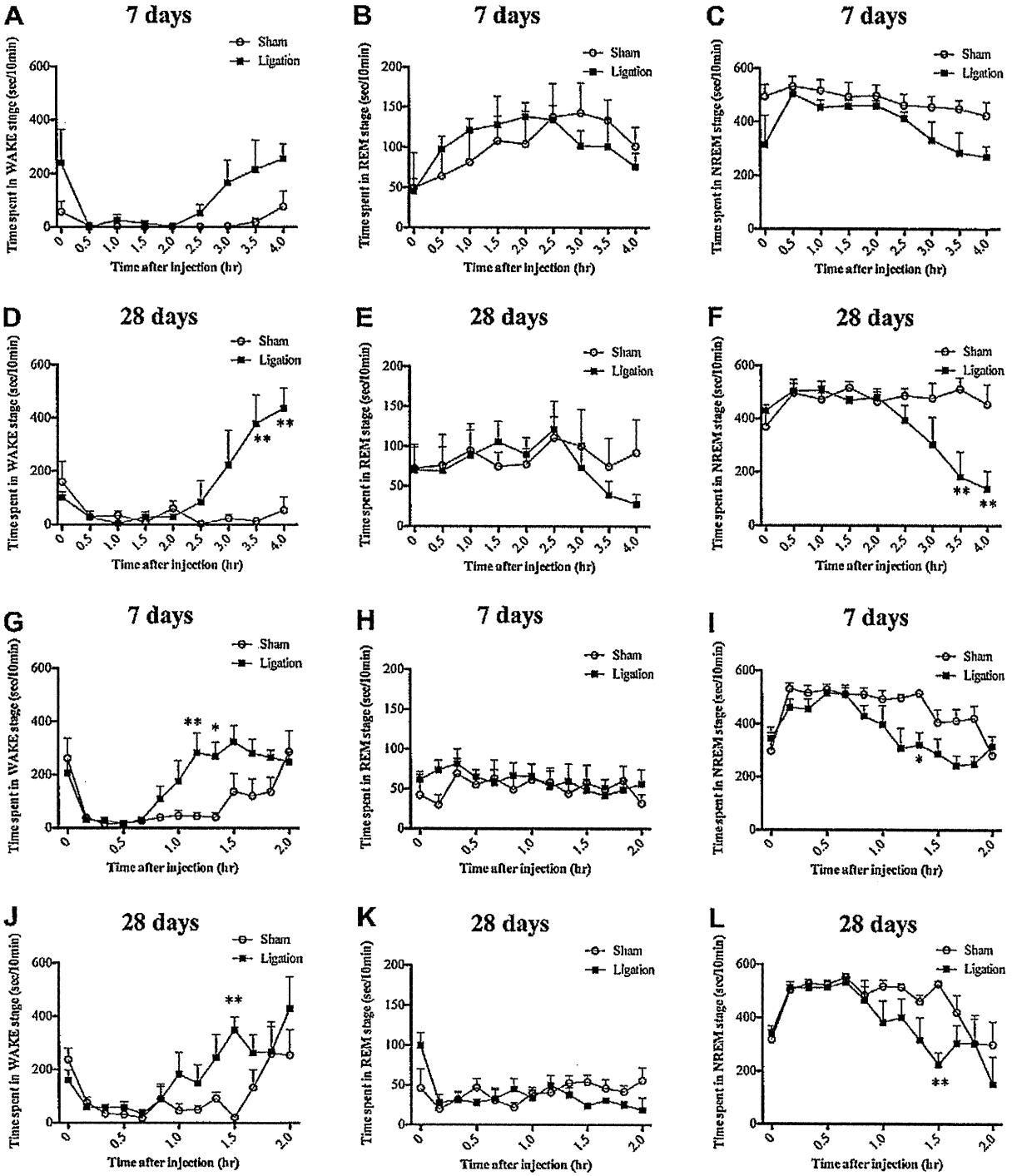

Fig. 9. Sleep–wake states after an i.p. injection of midazolam or zolpidem under a neuropathic pain-like state. At 7 days (A–C) or 28 days (D–F) after sciatic nerve ligation, mice were injected with midazolam (75 mg/kg, i.p.). The wake time was prolonged in mice with midazolam at 7 days (A) or 28 days (D) after sciatic nerve ligation. There were no changes in REM sleep induced by midazolam between sham-operated and nerve-ligated mice at 7 days (B) and 28 days (E). NREM sleep induced by midazolam was suppressed at 7 days (C) and 28 days (F) after sciatic nerve ligation. At 7 days (G–I) or 28 days (J–L) after sciatic nerve ligation, mice were injected with zolpidem (30 mg/kg, i.p.). The wake time was prolonged by zolpidem at 7 days (G) or 28 days (J) after sciatic nerve ligation. There were no changes in the REM sleep induced by zolpidem between sham-operated and nerve-ligated mice at 7 days (H) and 28 days (K). NREM sleep induced by zolpidem was suppressed at 7 days (I) or 28 days (L) after sciatic nerve ligation. One-way ANOVA was performed, followed by Bonferroni testing (unless otherwise indicated). Each point represents the mean ± SEM of 6 to 8 mice.

Fig. 8. Effects of midazolam, zolpidem and pentobarbital on the onset time of LORR and the LORR-time under a neuropathic pain-like state. At 7 days (A, C, and E) or 28 days (B, D, and F) after sciatic nerve ligation, mice were injected with midazolam (75 mg/kg, i.p.), zolpidem (30 mg/kg, i.p.) or pentobarbital (70 mg/kg, i.p.). The onset time of LORR induced by midazolam or zolpidem was significantly prolonged, whereas the LORR-time with midazolam or zolpidem was significantly shortened in mice at 7 or 28 days after sciatic nerve ligation. Each column represents the mean ± SEM, $^{*}P < .05$ and $^{**}P < .01$ vs sham group. The onset time of LORR and the LORR-time induced by zolpidem after the microinjection of SNAP-5114 (SNAP) into the cingulate cortex of nerve-ligated mice. At 7 days (G) or 28 days (H) after nerve ligation, mice were injected with zolpidem (30 mg/kg, i.p.) 3 h after the microinjection of vehicle or SNAP (1 nmol/mouse) into the cingulate cortex. Each bar represents the mean ± SEM of 6 to 9 mice. $^{*}P < 0.05$, $^{**}P < 0.01$, $^{***}P < 0.001$ vs vehicle-sham group, $^{\#}P < 0.05$, $^{\#\#\#}P < 0.001$ vs vehicle-ligation group.

but rather facilitate the action of endogenous GABA by increasing the frequency of channel-opening, whereas barbiturates can directly open $GABA_A$ receptor-associated chloride channels in the absence of GABA [5,26]. The LORR has been considered to be useful as a marker of the hypnotic state to investigate the sleep effects induced by benzodiazepines. In the present study, we documented that the LORR effects induced by i.p. administration of midazolam and zolpidem, both of which require endogenous GABA to produce their hypnotic effects, were significantly attenuated by sciatic nerve ligation. Furthermore, on the basis of the results of EEG/EMG, midazolam and zolpidem reduced the amount of wakefulness and increased the amount of NREM sleep in sham-operated mice. These effects were dramatically suppressed in mice with sciatic nerve ligation. To further ascertain the specific involvement of GAT-3 in the reduction of GABAergic transmission under a neuropathic pain-like state, we next investigated the effects of the microinjection of SNAP-5114 on the hypnotic effects of zolpidem in mice with sciatic nerve ligation. In this study, the prolonged onset time of LORR and shortened LORR-time by midazolam in nerve-ligated mice was completely reversed to the normal level by the intracingulate cortex injection of SNAP-5114. In contrast, the onset time of LORR and the duration of LORR induced by the i.p. injection of pentobarbital, which can induce its effect without GABA, in sciatic nerve-ligated mice were similar to those in sham-operated mice. These findings support the idea that nerve injury may decrease inhibitory GABAergic transmission in the cingulate cortex, possibility leading to suppression of the hypnotic effects induced by benzodiazepines in mice with sciatic nerve ligation.

It is well recognized that the GABAergic system plays an important role in nociceptive processing in the spinal cord. A large proportion of GABA-A receptor-mediated neural inhibition occurs via postsynaptic action on spinal dorsal horn neurons [7,12,23,51,57,62]. An important factor that could lead to the development of neuropathic pain is the reduced inhibition, or disinhibition, of spinal cord neurons [13,52,60]. Changes in GABA receptor disinhibition in the spinal cord may arise from the reduced expression of potassium-chloride cotransporter 2 (KCC2) after peripheral nerve injury [10]. Considering these findings, we cannot deny the possibility that, like released GABA, postsynaptic GABA receptor function in the cingulate cortex could also be changed by neuropathic pain, which might be responsible for the insomnia and lower sensitivity to benzodiazepines as a result of chronic pain.

In conclusion, we have demonstrated that neuropathic pain may decrease the level of released GABA at the synaptic cleft in the mouse cingulate cortex associated with an increase in GABA uptake through increased GATs on astrocytes, which results in the suppression of GABAergic transmission in the cingulate cortex region. Although further clarification is needed, we propose that this phenomenon may at least partly explain sleep dysregulation under a neuropathic pain.

Conflict of interest statement

The authors have no conflicts of interest to report.

Acknowledgments

This work was supported by a Grant-in-Aid for Scientific Research and a research grant from the Ministry of Education, Culture, Sports, Science and Technology of Japan. We thank Dr Keisuke Hashimoto and Shigemi Takagi for their expert technical assistance. The present study was conducted in accordance with the Guiding Principles for the Care and Use of Laboratory Animals, Hoshi University, as adopted by the Committee on Animal Research of Hoshi University.

References

[1] Andersen ML, Tufik S. Sleep patterns over 21-day period in rats with chronic constriction of sciatic nerve. Brain Res 2003;984:84–92.
[2] Bateson AN. The benzodiazepine site of the GABAA receptor: an old target with new potential? Sleep Med 2004;5:S9–S15.
[3] Borden LA, Dhar TG, Smith KE, Branchek TA, Gluchowski C, Weinshank RL. Cloning of the human homologue of the GABA transporter GAT-3 and identification of a novel inhibitor with selectivity for this site. Receptors Channels 1994;2:207–13.
[4] Borden LA, Smith KE, Hartig PR, Branchek TA, Weinshank RL. Molecular heterogeneity of the gamma-aminobutyric acid (GABA) transport system. Cloning of two novel high affinity GABA transporters from rat brain. J Biol Chem 1992;267:21098–104.
[5] Bormann J. Electrophysiology of GABAA and GABAB receptor subtypes. Trends Neurosci 1988;11:112–6.
[6] Bradford MM. A rapid and sensitive method for the quantitation of microgram quantities of protein utilizing the principle of protein–dye binding. Anal Biochem 1976;72:248–54.
[7] Brown AG, Koerber HR, Noble R. An intracellular study of spinocervical tract cell responses to natural stimuli and single hair afferent fibres in cats. J Physiol 1987;382:331–54.
[8] Casey KL. Forebrain mechanisms of nociception and pain: analysis through imaging. Proc Natl Acad Sci USA 1999;96:7668–74.
[9] Clark JA, Deutch AY, Gallipoli PZ, Amara SG. Functional expression and CNS distribution of a beta-alanine-sensitive neuronal GABA transporter. Neuron 1992;9:337–48.
[10] Coull JA, Boudreau D, Bachand K, Prescott SA, Nault F, Sik A, De Koninck P, De Koninck Y. Trans-synaptic shift in anion gradient in spinal lamina I neurons as a mechanism of neuropathic pain. Nature 2003;424:938–42.
[11] Danbolt NC. The high affinity uptake system for excitatory amino acids in the brain. Prog Neurobiol 1994;44:377–96.
[12] De Koninck Y, Henry JL. Prolonged GABAA-mediated inhibition following single hair afferent input to single spinal dorsal horn neurones in cats. J Physiol 1994;476:89–100.
[13] Dickenson AH. Balances between excitatory and inhibitory events in the spinal cord and chronic pain. Prog Brain Res 1996;110:225–31.
[14] Eisenberger NI, Lieberman MD, Williams KD. Does rejection hurt? An FMRI study of social exclusion. Science 2003;302:290–2.
[15] Foundation NS. Sleep in America: a national survey of US adults. Princeton, NJ: Gallup Organization; 1991.
[16] Franklin KBJ, Paxinos G. The mouse brain in stereotaxic coordinates. San Diego, California: Academic Press; 1997.
[17] Galer BS, Gianas A, Jensen MP. Painful diabetic polyneuropathy: epidemiology, pain description, and quality of life. Diabetes Res Clin Pract 2000;47:123–8.
[18] Galer BS, Henderson J, Perander J, Jensen MP. Course of symptoms and quality of life measurement in complex regional pain syndrome: a pilot survey. J Pain Symptom Manage 2000;20:286–92.
[19] Gerashchenko D, Wisor JP, Burns D, Reh RK, Shiromani PJ, Sakurai T, de la Iglesia HO, Kilduff TS. Identification of a population of sleep-active cerebral cortex neurons. Proc Natl Acad Sci USA 2008;105:10227–32.
[20] Gottesmann C. GABA mechanisms and sleep. Neuroscience 2002;111:231–9.
[21] Guastella J, Nelson N, Nelson H, Czyzyk L, Keynan S, Miedel MC, Davidson N, Lester HA, Kanner BI. Cloning and expression of a rat brain GABA transporter. Science 1990;249:1303–6.
[22] Haythornthwaite JA, Hegel MT, Kerns RD. Development of a sleep diary for chronic pain patients. J Pain Symptom Manage 1991;6:65–72.
[23] Hongo T, Jankowska E, Lundberg A. Convergence of excitatory and inhibitory action on interneurones in the lumbosacral cord. Exp Brain Res 1966;1:338–58.
[24] Huang ZL, Qu WM, Eguchi N, Chen JF, Schwarzschild MA, Fredholm BB, Urade Y, Hayaishi O. Adenosine A2A, but not A1, receptors mediate the arousal effect of caffeine. Nat Neurosci 2005;8:858–9.
[25] Huang ZL, Qu WM, Li WD, Mochizuki T, Eguchi N, Watanabe T, Urade Y, Hayaishi O. Arousal effect of orexin A depends on activation of the histaminergic system. Proc Natl Acad Sci USA 2001;98:9965–70.
[26] Inomata N, Tokutomi N, Oyama Y, Akaike N. Intracellular picrotoxin blocks pentobarbital-gated Cl^- conductance. Neurosci Res 1988;6:72–5.
[27] Iversen LL. Role of transmitter uptake mechanisms in synaptic neurotransmission. Br J Pharmacol 1971;41:571–91.
[28] Iversen LL, Kelly JS. Uptake and metabolism of gamma-aminobutyric acid by neurones and glial cells. Biochem Pharmacol 1975;24:933–8.
[29] Iversen LL, Neal MJ. The uptake of [3H]GABA by slices of rat cerebral cortex. J Neurochem 1968;15:1141–9.
[30] Iversen LL, Snyder SH. Synaptosomes: different populations storing catecholamines and gamma-aminobutyric acid in homogenates of rat brain. Nature 1968;220:796–8.
[31] Koyama T, Kato K, Mikami A. During pain-avoidance neurons activated in the macaque anterior cingulate and caudate. Neurosci Lett 2000;283:17–20.
[32] Kuzumaki N, Narita M, Hareyama N, Niikura K, Nagumo Y, Nozaki H, Amano T, Suzuki T. Chronic pain-induced astrocyte activation in the cingulate cortex with no change in neural or glial differentiation from neural stem cells in mice. Neurosci Lett 2007;415:22–7.
[33] Lavigne G, Sessle B, Choiniere M, Soja P. Sleep and pain. Seatle, WA: IASP Press; 2007.

[34] Lawrence CC, Gilbert CJ, Peters WP. Evaluation of symptom distress in a bone marrow transplant outpatient environment. Ann Pharmacother 1996;30:941–5.
[35] Li Q, Lau A, Morris TJ, Guo L, Fordyce CB, Stanley EF. A syntaxin 1, Galpha(o), and N-type calcium channel complex at a presynaptic nerve terminal: analysis by quantitative immunocolocalization. J Neurosci 2004;24:4070–81.
[36] Liu QR, Lopez-Corcuera B, Mandiyan S, Nelson H, Nelson N. Molecular characterization of four pharmacologically distinct gamma-aminobutyric acid transporters in mouse brain. J Biol Chem 1993;268:2106–12.
[37] Matthies HJ, Moore JL, Saunders C, Matthies DS, Lapierre LA, Goldenring JR, Blakely RD, Galli A. Rab11 supports amphetamine-stimulated norepinephrine transporter trafficking. J Neurosci 2010;30:7863–77.
[38] Moffitt PF, Kalucy EC, Kalucy RS, Baum FE, Cooke RD. Sleep difficulties, pain and other correlates. J Intern Med 1991;230:245–9.
[39] Morin CM, Gibson D, Wade J. Self-reported sleep and mood disturbance in chronic pain patients. Clin J Pain 1998;14:311–4.
[40] Narita M, Kuzumaki N, Kaneko C, Hareyama N, Miyatake M, Shindo K, Miyoshi K, Nakajima M, Nagumo Y, Sato F, Wachi H, Seyama Y, Suzuki T. Chronic pain-induced emotional dysfunction is associated with astrogliosis due to cortical delta-opioid receptor dysfunction. J Neurochem 2006;97:1369–78.
[41] Narita M, Kuzumaki N, Miyatake M, Sato F, Wachi H, Seyama Y, Suzuki T. Role of delta-opioid receptor function in neurogenesis and neuroprotection. J Neurochem 2006;97:1494–505.
[42] Narita M, Mizoguchi H, Nagase H, Suzuki T, Tseng LF. Involvement of spinal protein kinase Cgamma in the attenuation of opioid mu-receptor-mediated G-protein activation after chronic intrathecal administration of [d-Ala2, N-MePhe4, Gly-Ol(5)]enkephalin. J Neurosci 2001;21:3715–20.
[43] Narita M, Mizuo K, Mizoguchi H, Sakata M, Tseng LF, Suzuki T. Molecular evidence for the functional role of dopamine D3 receptor in the morphine-induced rewarding effect and hyperlocomotion. J Neurosci 2003;23:1006–12.
[44] Narita M, Nagumo Y, Hashimoto S, Khotib J, Miyatake M, Sakurai T, Yanagisawa M, Nakamachi T, Shioda S, Suzuki T. Direct involvement of orexinergic systems in the activation of the mesolimbic dopamine pathway and related behaviors induced by morphine. J Neurosci 2006;26:398–405.
[45] Narita M, Usui A, Niikura K, Nozaki H, Khotib J, Nagumo Y, Yajima Y, Suzuki T. Protease-activated receptor-1 and platelet-derived growth factor in spinal cord neurons are implicated in neuropathic pain after nerve injury. J Neurosci 2005;25:10000–9.
[46] Neal MJ, Iversen LL. Subcellular distribution of endogenous and (3H) gamma-aminobutyric acid in rat cerebral cortex. J Neurochem 1969;16:1245–52.
[47] Nicholson B, Verma S. Comorbidities in chronic neuropathic pain. Pain Med 2004;5:S9–S27.
[48] Radian R, Bendahan A, Kanner BI. Purification and identification of the functional sodium- and chloride-coupled gamma-aminobutyric acid transport glycoprotein from rat brain. J Biol Chem 1986;261:15437–41.
[49] Rainville P, Bushnell MC, Duncan GH. Representation of acute and persistent pain in the human CNS: potential implications for chemical intolerance. Ann NY Acad Sci 2001;933:130–41.
[50] Rainville P, Duncan GH, Price DD, Carrier B, Bushnell MC. Pain affect encoded in human anterior cingulate but not somatosensory cortex. Science 1997;277:968–71.
[51] Salter MW, De Koninck Y, Henry JL. Physiological roles for adenosine and ATP in synaptic transmission in the spinal dorsal horn. Prog Neurobiol 1993;41:125–56.
[52] Sandkuhler J. Neurobiology of spinal nociception: new concepts. Prog Brain Res 1996;110:207–24.
[53] Smith MT, Perlis ML, Smith MS, Giles DE, Carmody TP. Sleep quality and presleep arousal in chronic pain. J Behav Med 2000;23:1–13.
[54] Takayama C, Inoue Y. Developmental expression of GABA transporter-1 and -3 during formation of the GABAergic synapses in the mouse cerebellar cortex. Brain Res Dev Brain Res 2005;158:41–9.
[55] Talbot JD, Marrett S, Evans AC, Meyer E, Bushnell MC, Duncan GH. Multiple representations of pain in human cerebral cortex. Science 1991;251:1355–8.
[56] Tobler I, Deboer T, Fischer M. Sleep and sleep regulation in normal and prion protein-deficient mice. J Neurosci 1997;17:1869–79.
[57] Todd AJ, Spike RC. The localization of classical transmitters and neuropeptides within neurons in laminae I–III of the mammalian spinal dorsal horn. Prog Neurobiol 1993;41:609–45.
[58] Wang LE, Bai YJ, Shi XR, Cui XY, Cui SY, Zhang F, Zhang QY, Zhao YY, Zhang YH. Spinosin, a C-glycoside flavonoid from semen Zizhiphi Spinozae, potentiated pentobarbital-induced sleep via the serotonergic system. Pharmacol Biochem Behav 2008;90:399–403.
[59] Widerstrom-Noga EG, Felipe-Cuervo E, Yezierski RP. Chronic pain after spinal injury: interference with sleep and daily activities. Arch Phys Med Rehabil 2001;82:1571–7.
[60] Wiesenfeld-Hallin Z, Aldskogius H, Grant G, Hao JX, Hokfelt T, Xu XJ. Central inhibitory dysfunctions: mechanisms and clinical implications. Behav Brain Sci 1997;20:420–5.
[61] Xu H, Wu LJ, Wang H, Zhang X, Vadakkan KI, Kim SS, Steenland HW, Zhuo M. Presynaptic and postsynaptic amplifications of neuropathic pain in the anterior cingulate cortex. J Neurosci 2008;28:7445–53.
[62] Yoshimura M, Nishi S. Blind patch-clamp recordings from substantia gelatinosa neurons in adult rat spinal cord slices: pharmacological properties of synaptic currents. Neuroscience 1993;53:519–26.
[63] Zhao MG, Ko SW, Wu LJ, Toyoda H, Xu H, Quan J, Li J, Jia Y, Ren M, Xu ZC, Zhuo M. Enhanced presynaptic neurotransmitter release in the anterior cingulate cortex of mice with chronic pain. J Neurosci 2006;26:8923–30.

分担研究者　白石成二

研究成果の刊行に関する一覧表

書籍

著者氏名	論文タイトル名	書籍全体の編集者名	書　籍　名	出版社名	出版地	出版年	ページ

雑誌

発表者氏名	論文タイトル名	発表誌名	巻号	ページ	出版年
Onizuka S, Shiraishi S, Tamura R, Yonaha T, Oda N, Kawasaki Y, Syed NI, Shirasaka T, Tsuneyoshi I.	Lidocaine tratment during synapse reformation periods permanently inhibits NGF-induced excitation in an identified reconstructed synapse of Lymnaea stagnalis.	J Anesth	26 (1)	45-53	2012
Onizuka S, Tamura R, Yonaha T, Oda N, Kawasaki Y, Shirasaka T, Shiraishi S, Tsuneyoshi I.	Clinical dose of lidocaine destroys the cell membrane and induces both necrosis and epoptosis in an identified Lymnaea neuron.	J Anesth	26 (1)	54-61	2012
Yokoyama T, Minami K, Sudo Y, Horishita T, Ogata J, Yanagita T, Uezono Y.	Effects of sevoflurane on voltage-gated sodium channel $Na_v1.8$, $Na_v1.7$, and $Na_v1.4$ expressed in *Xenopus* oocytes.	J Anesth	25 (4)	609-613	2011
Minami K, Yokoyama T, Ogata J, Uezono Y.	The tramadol metabolite *O*-Desmethyl tramadol inhibits substance P-receptor functions expressed in *Xenopus* Oocytes.	J Pharmacol Sci	115 (3)	421-424	2011

Yanagita T, Satoh S, Uezono Y, Matsuo K, Nemoto T, Maruta T, Yoshikawa N, Iwakiri T, Minami K, Murakami M.	Transcriptional up-regulation of cell surface Nav1.7 sodium channels by insulin-like growth factor-1 via inhibition of glycogen synthase kinase-3β in adrenal chromaffin cells: enhancement of $^{22}Na^{+}$ influx, $^{45}Ca^{2+}$ influx and catecholamine secretion.	Neuropharmacology	61 (8)	1265-1274	2011
Minami K, Sudo Y, Yokoyama T, Ogata J, Takeuchi M, Uezono Y.	Sevoflurane inhibits the μ-opioid receptor function expressed in *Xenopus* oocytes.	Pharmacology	88 (3-4)	127-132	2011
Imai S, Sudo Y, Nakamura A, Ozeki A, Asato M, Hojo M, Devi LA, Kuzumaki N, Suzuki T, Uezono Y, Narita, M.	Possible involvement of β-endorphin in a loss of the coordinated balance of μ-opioid receptors trafficking processes by fentanyl.	Synapse	65 (9)	962-966	2011

J Anesth (2012) 26:45–53
DOI 10.1007/s00540-011-1257-6

ORIGINAL ARTICLE

Lidocaine treatment during synapse reformation periods permanently inhibits NGF-induced excitation in an identified reconstructed synapse of *Lymnaea stagnalis*

Shin Onizuka · Seiji Shiraishi · Ryuuji Tamura · Tetsu Yonaha · Nobuko Oda · Yuko Kawasaki · Naweed I. Syed · Tetsuro Shirasaka · Isao Tsuneyoshi

Received: 18 February 2011 / Accepted: 22 September 2011 / Published online: 30 October 2011

Abstract
Purpose Nerve growth factor (NGF) has been reported to affect synaptic transmission and cause neuropathic pain. In contrast, lidocaine has been used to reduce neuropathic pain; however, the effect of NGF and lidocaine on spontaneous transmitter release and synapse excitation has not been fully defined. Therefore, the effect of NGF and lidocaine on nerve regeneration, synapse reformation, and subsequent spontaneous transmitter release was investigated. We used *Lymnaea stagnalis* soma–soma-identified synaptic reconstruction to demonstrate that a transient increase in both frequency and amplitude of spontaneous events of miniature endplate potentials (MEPPs) occurs following NGF treatment and a short burst of action potentials in the presynaptic cell; in addition, the effect of lidocaine on NGF-induced synapse reformation was investigated.
Methods Using a cell culture and electrophysiological and FM-143 imaging techniques for exocytosis on unequivocally identified presynaptic visceral dorsal 4 (VD4) and postsynaptic somata left pedal (LPeE) neurons from the mollusc *Lymnaea stagnalis*, the effects of NGF and lidocaine on nerve regeneration, synapse reformation, and its electrophysiological spontaneous synaptic transmission between cultured neurons were described.
Results NGF increased axonal growth, frequency, and amplitudes of MEPPs. Lidocaine exposure during synapse reformation periods was drastically and permanently reduced axonal growth and the incidence of synapse excitation by NGF.
Conclusion NGF increased amplitudes and frequencies of MEPPs and induced synaptic excitation by increasing axonal growth and exocytosis. Lidocaine exposure during synapse reformation periods permanently suppressed NGF-induced excitation by suppressing axonal growth and exocytosis of presynaptic neurons in the identified reconstructed synapse of *L. stagnalis*.

Keywords Lidocaine · NGF · Apoptosis · Miniature endplate potentials

S. Onizuka (✉) · R. Tamura · T. Yonaha · N. Oda · Y. Kawasaki · T. Shirasaka · I. Tsuneyoshi
Department of Anesthesiology and Intensive Care, Faculty of Medicine, University of Miyazaki, Kiyotake-Cho, Miyazaki 889-1692, Japan
e-mail: pirotann@med.miyazaki-u.ac.jp

S. Shiraishi
Innovative Pathophysiology Research Group, Division of Cancer Pathophysiology, National Cancer Center Research Institute, 5-1-1 Tsukiji, Chuo-ku, Tokyo 104-0045, Japan

N. I. Syed
Faculty of Medicine, Calgary Brain Institute, University of Calgary, Calgary, AB, Canada

Introduction

Nerve growth factor (NGF) regulates survival, growth, or differentiation of a discrete population of neurons and is involved in neural plasticity. NGF transmits its signals intracellularly via a specific member of the trk family of receptor tyrosine kinases, trkA [1]. NGF not only is critical for the survival of a population of sensory neurons during their development but plays a role in maintaining phenotypes of adult dorsal-root ganglion (DRG) neurons [2]. Therefore, NGF is critically involved in neuropathic pain, such as hyperalgesia [3]. As

neuropathic pain is often unresponsive to conventional analgesics such as opiates and nonsteroidal anti-inflammatory drugs, the choice of treatment has been largely limited. Local anesthetics block the activity of voltage-gated sodium channels, thereby reversibly inhibiting the conduction of nerve impulses along axons and neuron excitation [4]. Based on these mechanisms of action, local anesthetics can be used to reduce neuropathic pain in clinical practice. The amelioration of pain by these drugs sometimes outlasts the duration of the sodium (Na^+)-channel blockade, probably due to their pharmacological properties. Although the underlying mechanisms of this persistent analgesic effect are largely unknown, several hypotheses have been proposed: interrupting nociceptor activity with local anesthetics not only leads to reversible sensitization of spinal-cord neurons but might also induce plastic changes in neurons depending on the timing and period of exposure [5–7]. Identifying the mechanisms of action of local anesthetics to relieve chronic pain might lead to the development of a new strategy to treat neuropathic pain. Therefore, the aim of this study was to clarify the effects of NGF and lidocaine on synaptic excitation during synapse reformation. To clarify these effects, the synaptic regeneration system of *Lymnaea stagnalis* was used.

Materials and methods

Animals and cell culture

All animal experiments were approved by the Animal Care Committee of the University of Miyazaki. Specifically, individual dorsal ganglion neurons from laboratory-raised *L. stagnalis* (freshwater snail) were used at room temperature. The snails were deshelled and transferred to a sterile dissection dish in normal *Lymnaea* saline: [51.3 mM sodium chloride (NaCl), 1.7 mM potassium chloride (KCl), 4.1 mM calcium chloride ($CaCl_2$), 1.5 mM magnesium chloride ($MgCl_2$), and 5.0 mM *N*-2-hydroxyethylpiperazine-*N*-2-ethanesulfonic acid (HEPES), pH 8, with sodium hydroxide (NaOH)]. Ganglia were treated in a defined medium (DM) [a serum-free 50% Leibovitz L-15 medium (GIBCO-BRL Life Technologies, Burlington, Ontario, Canada) with added inorganic salts, 20 μg/ml of gentamicin, pH 7.9)] for 25 min with 0.2% trypsin type III (Sigma Chemical Co., St. Louis, MO, USA). Neurons were removed by gentle suction with a siliconized fine-polished pipette with a microforge with an outer diameter of 1.5 mm (IB-150 F, WPI, Sarasota, FL, USA). After this, the previsceral dorsal 4 (VD4) and the postsynaptic somata left pedal E (LPeE) were juxtaposed in a soma–soma configuration on poly-L-lysine dishes (Falcon Plastics, Los Angeles, CA, USA) containing 3 ml of the defined medium (DM) or the DM with 10 ng/ml NGF for 24 h before use [8].

Neurite outgrowth

To assess neuronal regeneration in the absence and presence of NGF and lidocaine, identified neurons were isolated the cell culture and plated on poly-L-lysine-coated dishes containing the DM with NGF or DM with NGF and each concentration of lidocaine for 24 h. Presynaptic VD4 and postsynaptic LPeE neurons were selected for neurite outgrowth and synapse formation assays [9]. Neuronal sprouting was assessed as described previously [7]. Specifically, only those neurons exhibiting outgrowth (multiple branches and active growth cones) equivalent to a diameter of five somata were considered as sprouted. To test the hypothesis that NGF promotes neurite regeneration and synapse reformation from isolated identified neurons, cells were cultured in DM either in the absence or presence of NGF and allowed to extend neurites. The extent of outgrowth was calculated as a function of maximum neurite length. Identified presynaptic VD4 neurons were cultured with or without NGF and lidocaine. Specifically, cells were paired in close proximity and allowed to extend neurites. We reasoned that if neurons regenerated their processes, then synapses would develop between the neurites that could then be detected morphologically or electrophysiologically.

Intracellular recording

To assess synaptic reformation in the absence and presence of NGF and lidocaine, the following neuronal activity was monitored using a two-channel intracellular recording [10–12]. Sample neurons were exposed with NGF and lidocaine for 24 h, and after washout in culture solutions, the following experiments were performed: A glass microelectrode with a filament and an outside diameter of 1.5 mm (TW150F-4, WPI) was filled with a KCl pipette solution consisting of 50 mM KCl, 10 mM HEPES, and 2 mM magnesium adenosine triphosphate (Mg-ATP), and the pH was clamped to 7.0 with potassium hydroxide (KOH), yielding a tip resistance of 20–30 MΩ. Electrical signals were amplified with a current–voltage clamp amplifier (Multiclamp-700A, Axon Instruments, CA, USA). For experimental control and data acquisition, an analog–digital and digital–analog converter (Digidata 1322A, Axon Instruments) was used. Data acquisition and analysis were conducted using p-clamp software (p-clamp 9, Axon Instruments). In the somata–somata synapse model between presynaptic VD4 and postsynaptic LPeE neuron, the action potentials in VD4 in the absence of NGF conditions (Fig. 3) generated a 1:1 excitatory postsynaptic potential (EPSP) in

LPeE, and these excitatory responses were mimicked by an exogenous acetylcholine (ACh) puff (at arrow), which was performed (80-ms pulses, 1–2 psi) by applying 1 μM acetylcholine directly to the synaptic site via a Pneumatic PicoPump (PV800; World Precision Instruments) pressure injector under a fast perfusion system. In each synapse model, EPSP and the ACh responses were measured. To determine whether spontaneous transmitter release could be modulated by presynaptic activity, miniature endplate potentials (MEPPs) were recorded before and after a brief burst of action potentials in the presynaptic VD4 (10–15 action potentials at 5–10 Hz) generated by a continuous depolarizing current injection (0.5–1 nA). The holding membrane potential of each VD4 and LPeE neuron was −100 mV.

FM1-43 imaging

Cells were incubated in 20 μM FM1-43 (Molecular Probes, Eugene, USA) for 10 min. The presynaptic cell (VD4) stimulated the generation of 100 action potentials (10 spikes/burst) by conventional electrophysiological techniques to facilitate the uptake of FM1-43 in cells that were paired overnight either in the presence or absence of NGF, as described previously [7]. The probe and cultured medium were then replaced with cold saline to prevent neuronal firing during the washout and to remove background fluorescence. Fluorescent images of the FM1-43-labeled cells were acquired using a TE-300 inverted microscope (Nikon, Tokyo, Japan). Excitation light was from a Xenon lamp, excitation filters (490/30 nm), a dichroic mirror (505 nm), and emission filters (570 nm long-pass filter or 610 nm). Phase and fluorescent images were captured with an EM-CCD camera (Imagem, Hamamatsu Photonics, Tokyo, Japan) connected to a computer running AQAcosmos (Hamamatsu Photonics, Shizuoka, Japan). pixels in the cross-section of the fixed area (200×150 μm^2) were integrated and measured with NIH image software [version 1.62, National Institutes of Health (NIH), Bethesda, MA, USA]. Cells were paired overnight either in the absence or presence of NGF and lidocaine. On day two, the cultured solution was replaced with normal saline containing the dye FM1-43. The dye was then washed away with normal saline, and images were acquired.

Statistical analysis

Parametric data are expressed as mean ± standard error (SE) and were analyzed for significance using one-way analysis of variance (ANOVA) with repeated measures and a Scheffe's post hoc test. Nonparametric data are expressed in percentages and were analyzed for significance using the χ^2 test. Significance was assumed if $P < 0.05$.

Results

Effects of NGF and lidocaine on neurite outgrowth of pre- and postsynaptic neurons and paired pre- and postsynaptic neurons

The addition of NGF to the DM (DM with NGF) significantly enhanced neuron outgrowth, as shown by increases in the length and axon density of cultured presynaptic VD4 and postsynaptic LPeE neurons, which were suppressed by lidocaine in a concentration-dependent manner. In DM with NGF, an increase of outgrowth by NGF was almost completely suppressed by lidocaine at 50 and 100 μM (VD4 neurite length: DM, 59 ± 39; NGF, 162 ± 49; lidocaine 0.01 mM, 136 ± 28; lidocaine 0.1 mM, 38 ± 23; lidocaine 1 mM, 15 ± 9; LPeE neurite length DM, 67 ± 48; DM with NGF (NGF), 195 ± 101; lidocaine 0.01 mM, 154 ± 73; lidocaine 0.1 mM, 28 ± 14; lidocaine 1 mM, 11 ± 5 μm) (Fig. 1a, b). In paired pre- and postsynaptic neurons, the addition of NGF also potentiated neurite regeneration and synapse reformation, as shown by an increase in neurite length and the number of collaterals of the isolated identified neurons. Lidocaine also suppressed the increase of both neurite length and number of collaterals in these paired pre- and postsynaptic neurons, both of which were completely suppressed by 50 and 100 μM lidocaine (neurite length of paired VD4 and LPeE: DM, 64 ± 66; DM with NGF, 354 ± 359; lidocaine 0.01 mM, 259 ± 265; lidocaine 0.1 mM, 79 ± 75; lidocaine 1 mM, 65 ± 62 μm) (Fig. 2a, b).

Electrophysiological change of identified paired pre- and postsynaptic neurons with or without NGF and lidocaine

In DM with NGF, EPSP in LPeE was significantly increased versus DM conditions, and the ACh response also increased significantly more than under the DM conditions ($p < 0.05$). In DM with NGF, lidocaine exposure during the synapse formation period significantly reduced the EPSP in a concentration-dependent manner ($p < 0.05$) ($n = 10$–11) (Fig. 3b). In DM with NGF, the ACh response in LPeE was reduced by lidocaine at a high concentration (100 μM).

A brief burst of action potentials in VD4 (10–15 action potentials at 5–10 Hz) generated by a continuous depolarizing current injection (marked by the projecting bar in the bottom trace in Fig. 4a) significantly increased both MEPP frequency ($p < 0.05$) (Fig. 4a upper trace, Fig. 4b upper graph) and amplitude ($p < 0.05$) (Fig. 4a upper trace, Fig. 4b lower graph) for at least 1 min after cessation of the presynaptic action potential activity in the presence of NGF. In contrast, after the ACh puff in which the main

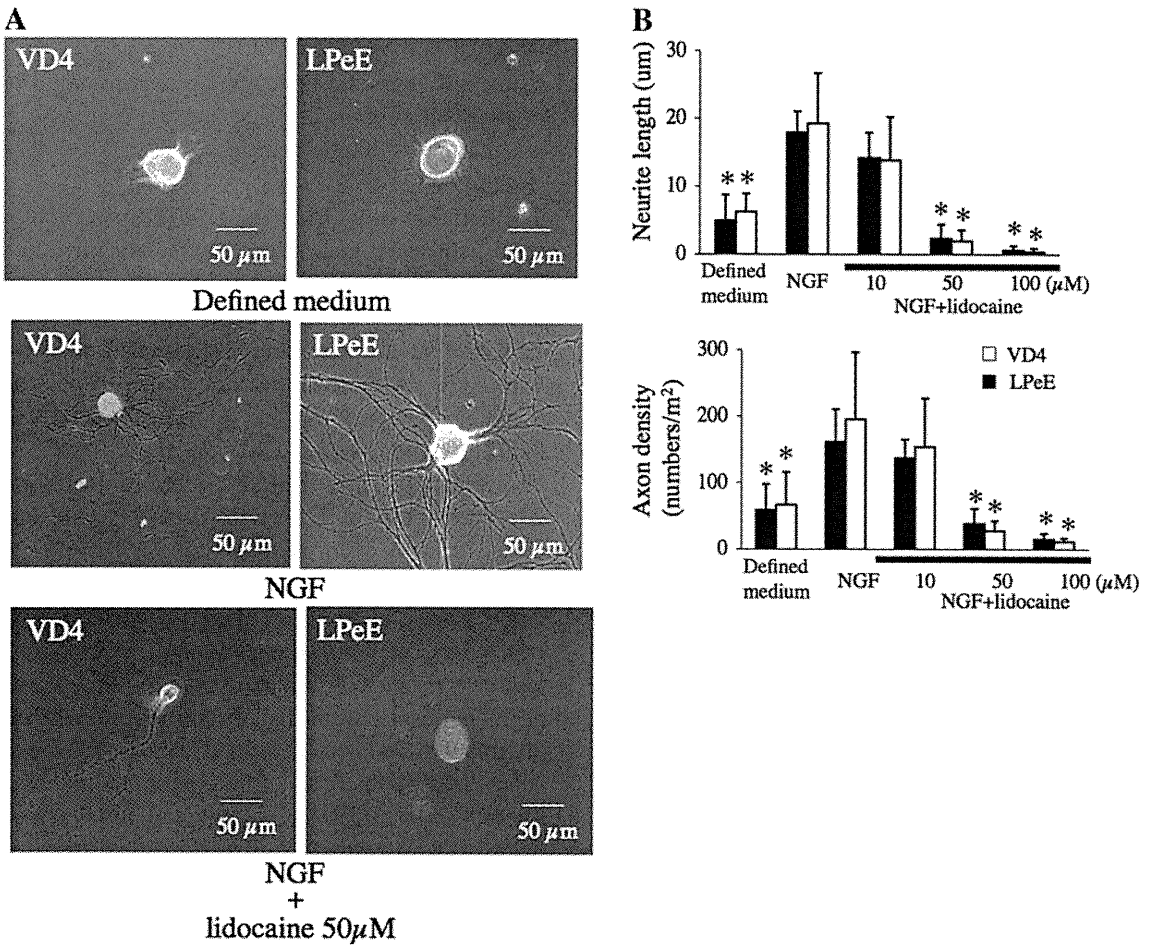

Fig. 1 Effects of nerve growth factor (NGF) and lidocaine on neurite regressions of presynaptic visceral dorsal 4 (VD4) cells. **a** To test the effects of NGF on neurite regeneration, presynaptic VD4 cells and postsynaptic somata left pedal (LPeE) cells were isolated and cultured in a defined culture medium (DM) either in the absence (*upper pictures*) ($n = 11$ in VD4 and $n = 7$ in LPeE) or presence (*middle pictures*) ($n = 13$ in VD4 and $n = 7$ in LPeE) of NGF and then exposed to lidocaine in the presence of NGF for 24 h during synapse reformation periods (*lower pictures*) ($n = 11$ in VD4 and $n = 7$ in LPeE). **b** NGF increased neurite outgrowth extensively. The growth exhibited in the presence of NGF was indistinguishable from that observed in the group without NGF. $*p < 0.05$ compared with the NGF group

transmitter of this synapse was exposed to the postsynaptic LPeE neuron, these MEPPs were not observed (Fig. 4a lower trace, Fig. 4b).

In DM with NGF, both MEPP frequency and amplitude increased significantly more than in the absence of NGF ($p < 0.05$) (Fig. 4c, d), and lidocaine exposure during the synapse reformation period significantly suppressed both MEPP frequency ($p < 0.05$) (Fig. 4c lower trace and Fig. 4d upper graph) and amplitude for at least 1 min after the cessation of presynaptic action potential activity in a concentration-dependent manner ($p < 0.05$) ($n = 11$–13) (Fig. 4c, d).

Exocytosis imaging by FM1-43

In DM with NGF, exclusive labeling of presynaptic cells was discernable at its contact site with LPeE as well as in its processes surrounding the postsynaptic somata (Fig. 5a). In contrast, faint staining of presynaptic cells was observed in VD4 paired in DM with NGF and lidocaine. The pixel values for each category were converted into 3D images by NIH imaging. They are depicted in the corresponding panels, their pixel values are calculated, and summaries are presented in Fig. 5b. In contrast, lidocaine inhibits NGF-promoted nerve regeneration and synapse formation in a concentration-dependent manner, as shown in Fig. 5.

Discussion

Study results demonstrate that NGF promoted neurite outgrowth (Figs. 1, 2) and EPSP amplitudes in response to ACh (Fig. 3) and generated spontaneous MEPPs (Fig. 4).

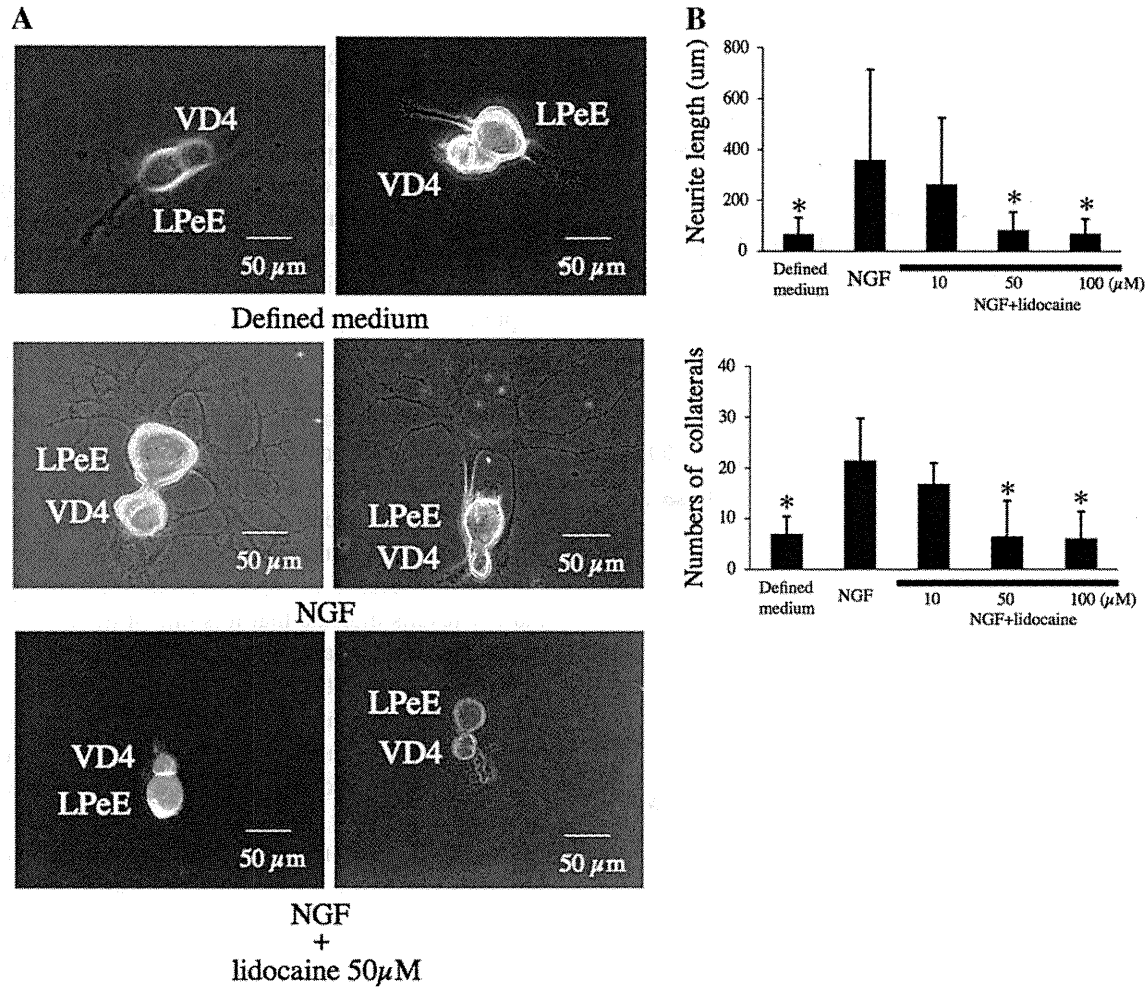

Fig. 2 Effects of nerve growth factor (NGF) and lidocaine on neurite regression in synaptic reconstitution. **a** To test the effects of NGF on neurite regeneration in synapse reconstruction, identified presynaptic visceral dorsal 4 (VD4) and postsynaptic somata left pedal (LPeE) neurons were isolated and cultured with their respective stomata in a defined culture medium (DM) either in the absence (*upper pictures*) ($n = 12$) or presence (*middle pictures*) ($n = 16$) of NGF. Lidocaine exposure for 24 h during synapse reformation periods suppressed NGF-induced neurite outgrowth (*lower pictures*) ($n = 14$). **b** NGF also increased neurite outgrowth extensively in synapse reconstruction; however, the growth exhibited in the presence of NGF was indistinguishable from that of the group without NGF. $*p < 0.05$ compared with NGF group

In contrast, lidocaine suppressed these NGF-promoted neurite outgrowths, EPSP, and MEPPs. Vesicles that include neurotransmitters, such as ACh, for synaptic transmission, as imaged by FM1-43, were stained much more in the presence of NGF than those of NGF with lidocaine, as shown in Fig. 5.

In general, an EPSP is a temporary depolarization of postsynaptic membrane potential caused by the flow of positively charged ions, such as sodium and calcium, into the postsynaptic cell as a result of opening of ligand-sensitive channels, such as the ACh receptor in postsynaptic cells by neurotransmitter stimulation, e.g., ACh, released from presynaptic cells by depolarization of the presynaptic cell. On the other hand, MEPPs are caused by spontaneous leakage of presynaptic neurotransmitter molecules, such as vesicles containing ACh, and MEPP amplitude depends on the amount of neurotransmitter leakage and postsynaptic response to them [13, 14]. Occasionally, ACh is likely to be spontaneously released because there is a basal level of calcium in the presynaptic terminal. Each vesicle, e.g., the vesicular ACh transporter, indeed contains enough transmitters to open >1,000 individual ACh-sensitive channels. Each vesicle refers to those small endplate potentials that occur randomly in the absence of any stimulation. EPSP is due to the summation effects of many vesicles being released at the same time by stimulation, such as action potential. One vesicle produces a potential of about 0.5 mV. The release of 100 of those vesicles at the same time could produce a potential that is 100 times as great (50 mV). Neurotransmitter (ACh) release for EPSP

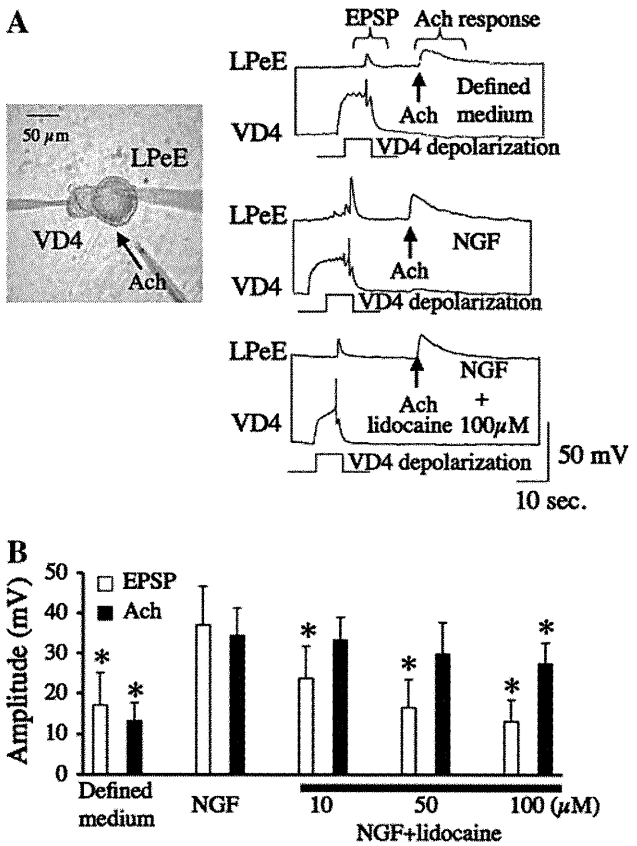

Fig. 3 Effects of nerve growth factor (NGF) and lidocaine on excitatory postsynaptic potential (EPSP) and response to acetylcholine (ACh). **a** Intracellular recordings between visceral dorsal 4 (VD4) and somata left pedal (LPeE) revealed an excitatory synapse in defined culture medium (DM), and the action potentials in the presynaptic cell generated 1:1 EPSP (*upper trace*). These excitatory responses were mimicked by exogenously applied ACh (*arrow*), which generated a compound EPSP. Both synaptic (VD4) and nonsynaptic (ACh) responses were significantly increased by NGF treatment (*middle trace*). VD4 responses were significantly depressed by lidocaine exposure during synapse reformation periods (*lower trace*). In contrast, nonsynaptic (ACh) responses were not suppressed by lidocaine treatment. **b** Results are presented as mean ± standard deviation, $n = 11$. $^*p < 0.05$ compared with NGF group

and MEPPs is triggered by intracellular Ca. Therefore, afterburst spikes increase intracellular Ca through voltage-dependent Ca channels, which will increase the amplitude and frequency of MEPPs. Our data also demonstrated that MEPPs were increased in both amplitude and frequency by a burst of presynaptic neurons but were not induced by ACh exposure to postsynaptic (LPeE) neurons, as shown in Fig. 4a, b. Therefore, these MEPP afterburst spikes in this VD4–LPeE synapse model are mainly dependent on the amount of neurotransmitter leakage from presynaptic neurons. Morphologically, the amplitude and frequency of MEPPs increased in the synapses, which have a high density of axons, as shown in Figs. 2 and 5. In FM1-43 imaging, which stains the exocytosis area, under NGF conditions, exclusive labeling of presynaptic VD4 cells was discernable at its contact site with postsynaptic LPeE. In addition, in many cells, the processes and axon collaterals surrounded the postsynaptic somata. It has been reported that NGF increases ACh synthesis and release and vesicular ACh transporter expression [15, 16].

Therefore, it is assumed that many input signals in postsynaptic neurons will be received from presynaptic neurons under NGF conditions and that mechanical inputs and presynaptic activity are important factors for MEPP amplitude and frequency. NGF treatment during synapse reformation periods significantly increased MEPP amplitude and frequency, especially after a burst of presynaptic neurons, as shown in Fig. 4c, d. These results suggest that NGF treatment during synapse reformation periods grows collateral axons that will increase neurotransmitter release from presynaptic neurons, which induces an increase in MEPP amplitude and frequency. In other words, NGF induces an increase in input sites of presynaptic signals, and our results indicate that it is one of the mechanisms of NGF-induced hyperalgesia.

We also demonstrate that long-term exposure to lidocaine during synapse reformation periods permanently suppresses EPSP and the MEPPs in both amplitude and frequency before and after a presynaptic neuron burst. We previously reported that lidocaine suppresses voltage-dependent Ca currents [12], and this is one reason that lidocaine suppresses both EPSP and the MEPPs, because these are triggered by Ca. Lidocaine also suppressed axon growth. Fujii et al. [17] reported that lidocaine suppressed ACh synthesis in 3T3 cells. Our investigation indicates that long-term exposure to lidocaine suppresses both EPSP and MEPP more than it suppresses ACh response in the postsynaptic neuron, and these results indicate that lidocaine suppresses neurotransmitter release from presynaptic neurons. Therefore, continuous exposure to lidocaine during synapse reformation periods will permanently suppress NGF-induced synaptic excitation, such as MEPPs, by reducing ACh synthesis and release and mechanical inputs from presynaptic to postsynaptic neurons.

Lidocaine has been shown in many reports to induce toxicity for axon degeneration [18–20]. Most of them indicate that lidocaine induces morphological changes in axons and neurons. We also reported that long-term exposure to lidocaine induced morphological changes in cone and neurite growth in *Lymnaea* neurons [21]. However, the mechanisms remain obscure. Marques et al. [22] reported that lidocaine changes the distribution of ACh receptors and induces long-term regeneration at the neuromuscular junction. Tsuchiya et al. [23] reported that lidocaine interacts with anionic phospholipid membrane structure dependently to modify fluidity and induces neuronal damage, such as apoptosis and necrosis. On the other hand, lidocaine has also been reported to act as a

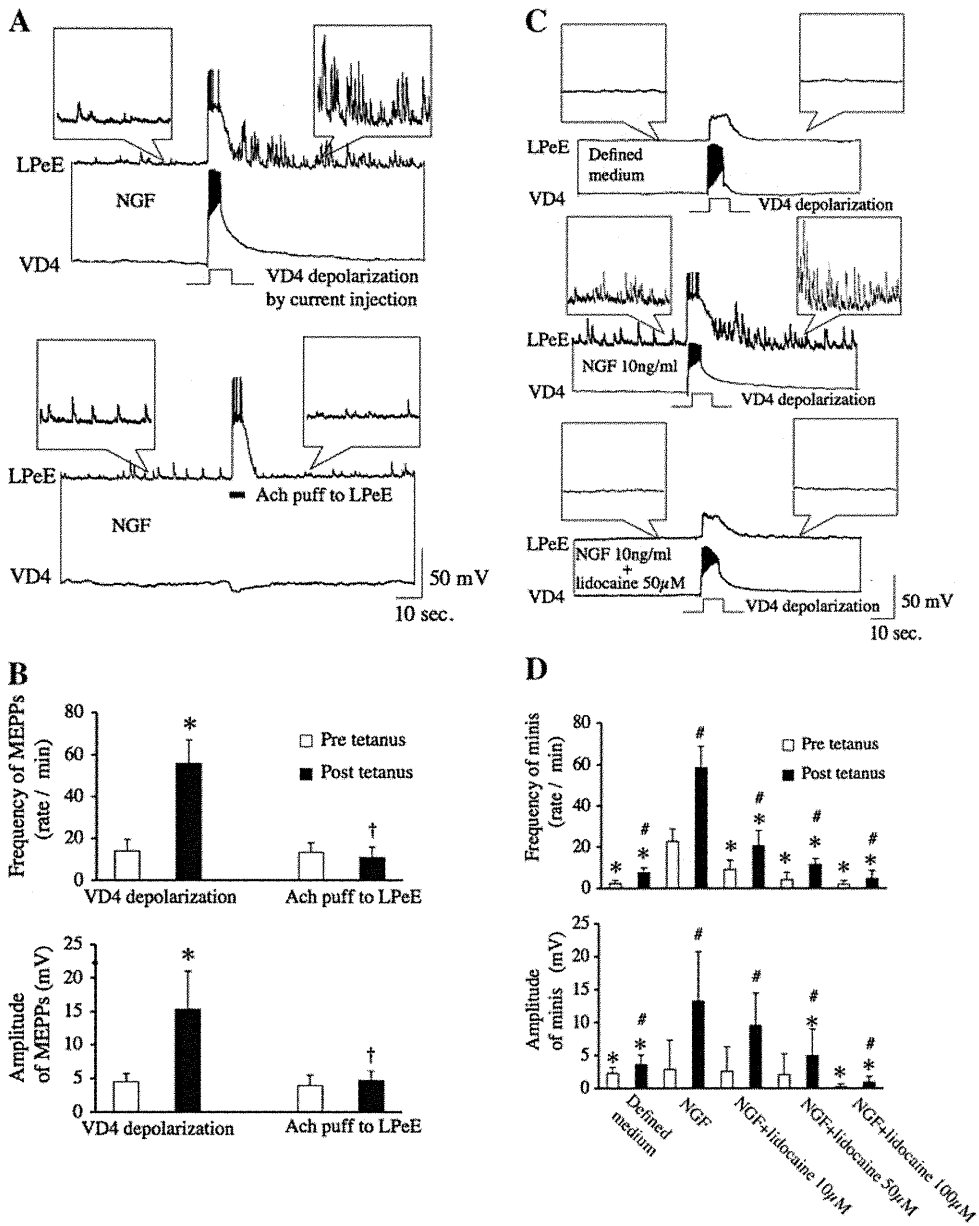

Fig. 4 Effects of nerve growth factor (NGF) and lidocaine on miniature endplate potentials (MEPPs). **a** Intracellular recordings between visceral dorsal 4 (VD4) and somata left pedal (LPeE) revealed an excitatory synapse in defined culture medium (DM) in the presence of NGF, and many MEPPs were observed by a brief burst of action potentials in VD4 (10–15 action potentials) generated by a continuous depolarizing current injection (*upper trace* of **a**). In contrast, following ACh puff to the postsynaptic LPeE neuron, these MEPPs were not obtained (*lower trace* of **a**). **b** *Upper graph* shows the frequency of MEPPs, and *lower trace* shows the amplitudes of MEPPs. Results are presented as the mean ± standard deviation, $n = 8$. *$p<0.05$ in comparison to baseline of pretetanus. $^{\dagger}p < 0.05$ compared with baseline. **c** Intracellular recordings between VD4 and LPeE revealed an excitatory synapse in DM in the absence of NGF; however, few MEPPs were observed (*upper trace*) ($n = 12$). In contrast, in the presence of NGF, many MEPPs were observed (*middle trace*) ($n = 14$). **d** A brief burst of action potentials in VD4 (10–15 action potentials) generated by a continuous depolarizing current injection significantly increased both MEPP frequency and amplitude for at least 1 min after cessation of presynaptic action potential activity. Lidocaine exposure during synapse reformation periods permanently inhibits these NGF-induced MEPPs (*lower trace*). **d** MEPP data. *Upper graph* shows the frequency of MEPPs, and the *lower trace* shows the amplitudes of MEPPs. Results are presented as mean ± standard deviation. *$p < 0.05$ compared with NGF group. $^{\#}p < 0.05$ compared with pretetanus

multitargeting drug. Lirk et al. [24] reported that lidocaine-induced axonal injury is caused by activation of the p38 mitogen-activated protein kinase. Radwan et al. [25] reported similar results; however, they presented a contrasting view in which the growth cone-collapsing effect of lidocaine on DRG neurons is reversed by several neurotrophic factors, such as NGF. Takatori et al. [26] reported identical results to ours, namely, that lidocaine

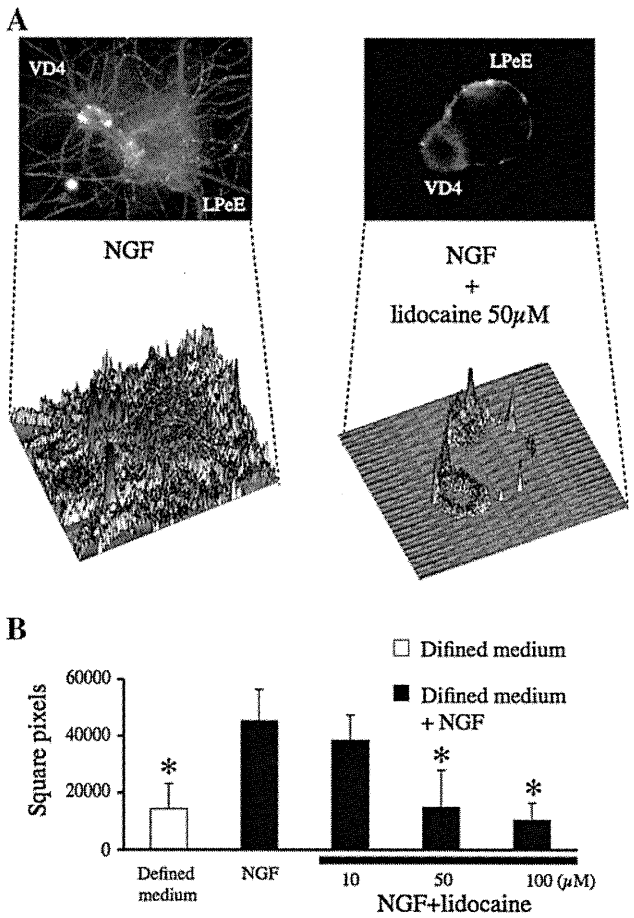

Fig. 5 Effects of nerve growth factor (NGF) and lidocaine on exocytotic profiles. **a** To test whether the transmitter secretory machinery of the presynaptic cell paired overnight in NGF was perturbed, the exocytotic profiles were analyzed through FM1-43 imaging. Visceral dorsal 4 (VD4) cells paired with somata left panel (LPeE) overnight in the presence of NGF (*left-hand pictures*) and NGF with lidocaine (*right-hand pictures*) and recorded under normal saline conditions were loaded with the FM1-43 dye. VD4 was extensively loaded either at its contact site with postsynaptic neurons (LPeE) or in its processes surrounding the postsynaptic somata (*left-hand pictures*). Lidocaine significantly decreased this NGF-induced axonal growth (*right-hand pictures*). *Corresponding panels under each image* represent 3D images of pixel values, **b** and these pixel values are averaged in a *bar graph*. Results are presented as mean ± standard deviation; $n = 8$–10. $^*p < 0.05$ compared with NGF group

suppresses NGF-mediated neurite outgrowth by inhibiting tyrosine kinase A activity. Our results demonstrate that lidocaine exposure during synapse reformation periods is able to suppress NGF-induced MEPPs permanently. Neurotrophic factors, such as NGF, have been reported to act as protein kinase A (PKA) because the inhibitor for PKA was able to inhibit synapse reformation within 24 h. In other words, these messengers of cyclic adenosine monophosphate (cAMP)-PKA pathway may play a novel role in regulating the synaptic efficacy during early synaptogenesis and plasticity induced by neurotrophic factors [27].

NGF is related to several types of neuropathic pain, such as herpetic neuralgia [28, 29], complex regional pain syndrome (CRPS) [30, 31], and cancer pain [32, 33]. In our investigation, we demonstrated that NGF increases MEPPs and induces excitation after synapse reformation, which will cause neuropathic pain, including hyperalgesia or allodynia. Hamakawa et al. [34] reported similar results in which the neurotrophic factor changes from an inhibitory synapse to excitatory synapse in the identified *Lymnaea* reconstructed synapse model. Therefore, lidocaine exposure in the early periods may be beneficial for treating these types of neuropathic pains [35].

In this experiment, human NGF was used. Human NGF is also able to support neurite outgrowth of *Lymnaea* neurons [9, 36]. We took advantage of an ideal model preparation in which synaptic transmission between uniquely identified neurons was investigated at the level of single pre- and postsynaptic neurons. Individually isolated neurons from the mollusc *Lymnaea* not only regenerate their neurites in cell culture but also recapitulate their specific patterns of synapses, which are similar to those observed in vivo.

It is very difficult to observe synaptic reformation morphologically and electrophysiologically in mammals in vivo because there are numerous glial cells and neurons of other cells obstructing the view. In contrast, the somata–somata synapse model of *Lymnaea* is the simplest, as it consists of only two pre- and postsynaptic neurons, which makes it easy to observe synaptic plasticity morphologically and electrophysiologically. Of course, there are species differences between *Lymnaea* and mammals; moreover, this somata–somata synapse model of *Lymnaea* provides a nice opportunity for synaptic plasticity. This in vitro approach using *Lymnaea* neurons has been extensively used in previous studies to decipher both cellular and synaptic mechanisms whereby NGF and various anesthetics affect neuronal function and synaptic transmission [9, 10, 16].

In conclusion, NGF increased axonal growth, EPSP amplitudes, and MEPP amplitudes and frequencies in the identified reconstructed synapse, and lidocaine exposure during synapse reformation periods permanently suppressed them in the identified reconstructed synapse of *L. stagnalis*.

Acknowledgments This work was supported in part by a Grant-in-Aid (No. 12770828) for Scientific Research (A) from The Ministry of Education, Science, and Technology of Japan.

References

1. McMahon SB, Bennett DLH, Bevan S. Inflammatory mediators and modulators of pain. In: McMahon SB, Koltzenburg M, editors. Wall and Melzack's textbook of pain. 5th ed. Philadelphia: Churchill Livingstone, 2005. p. 49–72.

2. Snider WD, McMahon SB. Tackling pain at the source: new ideas about nociceptors. Neuron. 1998;20:629–32.
3. Hefti FF, Rosenthal A, Walicke PA, Wyatt S, Vergara G, Shelton DL, Davies AM. Novel class of pain drugs based on antagonism of NGF. Trends Pharmacol Sci. 2006;27:85–91.
4. Catterall WA, Mackie K. Local anesthetics. In: Brunton LL, Lazo JS, Parker KL, editors. Goodman & Gilman's The pharmacological basis of therapeutics. 11th ed. New York: McGraw-Hill, 2006. p. 369–86.
5. Hogan QH, Abram SE. Neural blockade for diagnosis and prognosis. A review. Anesthesiology. 1997;86:216–41.
6. Smith LJ, Shih A, Miletic G, Miletic V. Continual systemic infusion of lidocaine provides analgesia in an animal model of neuropathic pain. Pain. 2002;97:267–73.
7. Onizuka S, Takasaki M, Syed NI. Long-term exposure to local but not inhalation anesthetics affects neurite regeneration and synapse formation between identified *Lymnaea* neurons. Anesthesiology. 2005;102:353–63.
8. Syed N, Bulloch A, Lukowiak K. In vitro reconstruction of the respiratory central pattern generator of the mollusk *Lymnaea*. Science. 1990;12:282–5.
9. Ridgway RL, Syed NI, Lukowiak K, Bulloch AGM. Nerve growth factor (NGF) induces sprouting of specific neurons of the snail, *Lymnaea stagnalis*. J Neurobiol. 1991;22:377–90.
10. Onizuka S, Kasaba T, Takasaki M. The effect of lidocaine on cholinergic neurotransmission in an identified reconstructed synapse. Anesth Analg. 2008;107:1236–42.
11. Woodin MA, Hamakawa T, Takasaki M, Lukowiak K, Syed NI. Trophic factor-induced plasticity of synaptic connections between identified *Lymnaea* neurons. Learn Mem. 1999;6:307–16.
12. Onizuka S, Kasaba T, Hamakawa T, Takasaki M. Lidocaine excites both pre- and postsynaptic neurons of reconstructed respiratory pattern generator in *Lymnaea stagnalis*. Anesth Analg. 2005;100:175–82.
13. Levitan I, Kaczmarek L. Synaptic release of neurotransmitters. In: The neuron. 3rd ed. Oxford University Press: Oxford. 2001; p. 196–200.
14. Boucher SD, Katz NL. Effects of several 'membrane stabilizing' agents on frog neuromuscular junction. Eur J Pharmacol. 1977;42:139–45.
15. Oosawa H, Fujii T, Kawashima K. Nerve growth factor increases the synthesis and release of acetylcholine and the expression of vesicular acetylcholine transporter in primary cultured rat embryonic septal cells. J Neurosci Res. 1999;57:381–7.
16. Takei N, Kuramoto H, Endo Y, Hatanaka H. NGF and BDNF increase the immunoreactivity of vesicular acetylcholine transporter in cultured neurons from the embryonic rat septum. Neurosci Lett. 1997;226:207–9.
17. Fujii T, Masai M, Misawa H, Okuda T, Takada-Takatori Y, Moriwaki Y, Haga T, Kawashima K. Acetylcholine synthesis and release in NIH3T3 cells coexpressing the high-affinity choline transporter and choline acetyltransferase. J Neurosci Res. 2009;87:3024–32.
18. Barrington MJ, Watts SA, Gledhill SR, Thomas RD, Said SA, Snyder GL, Tay VS, Jamrozik K. Preliminary results of the Australasian Regional Anaesthesia Collaboration: a prospective audit of more than 7000 peripheral nerve and plexus blocks for neurologic and other complications. Reg Anesth Pain Med. 2009;34:534–41.
19. Takenami T, Yagishita S, Asato F, Arai M, Hoka S. Intrathecal lidocaine causes posterior root axonal degeneration near entry into the spinal cord in rats. Reg Anesth Pain Med. 2002;27:58–67.
20. Hashimoto K, Sakura S, Bollen AW, Ciriales R, Drasner K. Comparative toxicity of glucose and lidocaine administered intrathecally in the rat. Reg Anesth Pain Med. 1998;23:444–50.
21. Kasaba T, Onizuka S, Takasaki M. Procaine and mepivacaine have less toxicity in vitro than other clinically used local anesthetics. Anesth Analg. 2003;97:85–90.
22. Marques MJ, Mendes ZT, Minatel E, Santo Neto H. Acetylcholine receptors and nerve terminal distribution at the neuromuscular junction of long-term regenerated muscle fibers. J Neurocytol. 2005;34:387–96.
23. Tsuchiya H, Ueno T, Mizogami M, Takakura K. Local anesthetics structure-dependently interact with anionic phospholipid membranes to modify the fluidity. Chem Biol Interact. 2010;183: 19–24.
24. Lirk P, Haller I, Colvin HP, Frauscher S, Kirchmair L, Gerner P, Klimaschewski L. In vitro, lidocaine-induced axonal injury is prevented by peripheral inhibition of the p38 mitogen-activated protein kinase, but not by inhibiting caspase activity. Anesth Analg. 2007;105:1657–64.
25. Radwan IA, Saito S, Goto F. Growth cone collapsing effect of lidocaine on DRG neurons is partially reversed by several neurotrophic factors. Anesthesiology. 2002;97:630–5.
26. Takatori M, Kuroda Y, Hirose M. Local anesthetics suppress nerve growth factor-mediated neurite outgrowth by inhibition of tyrosine kinase activity of TrkA. Anesth Analg. 2006;102:462–7.
27. Munno D, Prince D, Syed N. Synapse number and synaptic efficacy are regulated by presynaptic cAMP and protein kinase A. J Neurosci. 2003;23:4146–55.
28. Valderrama X, Rapin N, Misra V. Zhangfei, a novel regulator of the human nerve growth factor receptor, trkA. J Neurovirol. 2008;14:425–36.
29. Wolfe D, Goins WF, Kaplan TJ, Capuano SV, Fradette J, Murphey-Corb M, Robbins PD, Cohen JB, Glorioso JC. Herpesvirus-mediated systemic delivery of nerve growth factor. Mol Ther. 2001;3:61–9.
30. Sabsovich I, Wei T, Guo T, Zhao R, Shi X, Li X, Yeomans D, Klyukinov M, Kingery W, Clark J, Rukwied R. Mayer Effect of anti-NGF antibodies in a rat tibia fracture model of complex regional pain syndrome type I. Pain. 2008;138:47–60.
31. Kluschina O, Obreja O, Schley M, Schmelz M. NGF induces non-inflammatory localized and lasting mechanical and thermal hypersensitivity in human skin. Pain. 2010;148:407–13.
32. Halvorson KG, Kubota K, Sevcik MA, Lindsay TH, Sotillo JE, Ghilardi JR, Rosol TJ, Boustany L, Shelton DL, Mantyh PW. A blocking antibody to nerve growth factor attenuates skeletal pain induced by prostate tumor cells growing in bone. Cancer Res. 2005;65:9426–35.
33. Pierotti MA, Greco A. Oncogenic rearrangements of the NTRK1/NGF receptor. Cancer Lett. 2006;232:90–8.
34. Hamakawa T, Woodin M, Bjorgum M, Painter S, Takasaki M, Lukowiak K, Nagle G, Syed N. Excitatory synaptogenesis between identified *Lymnaea* neurons requires extrinsic trophic factors and is mediated by receptor tyrosine kinases. J Neurosci. 1999;19:9306–12.
35. Koppert W, Zeck S, Sittl R, Likar R, Knoll R, Schmelz M. Low-dose lidocaine suppresses experimentally induced hyperalgesia in humans. Anesthesiology. 1998;89:1345–53.
36. Wildering WC, Lodder JC, Kits KS, Bulloch AG. Nerve growth factor (NGF) acutely enhances high-voltage-activated calcium currents in molluscan neurons. J Neurophysiol. 1995;74:2778–81.

J Anesth (2012) 26:54–61
DOI 10.1007/s00540-011-1260-y

ORIGINAL ARTICLE

Clinical dose of lidocaine destroys the cell membrane and induces both necrosis and apoptosis in an identified *Lymnaea* neuron

Shin Onizuka · Ryuji Tamura · Tetsu Yonaha · Nobuko Oda · Yuko Kawasaki · Tetsuro Shirasaka · Seiji Shiraishi · Isao Tsuneyoshi

Received: 3 February 2011 / Accepted: 6 October 2011 / Published online: 29 October 2011

Abstract
Purpose Although lidocaine-induced cell toxicity has been reported, its mechanism is unclear. Cell size, morphological change, and membrane resistance are related to homeostasis and damage to the cell membrane; however, the effects of lidocaine on these factors are unclear. Using an identified LPeD1 neuron from *Lymnaea stagnalis*, we sought to determine how lidocaine affects these factors and how lidocaine is related to damage of the cell membrane.
Methods Cell size and morphological form were measured by a micrograph and imaging analysis system. Membrane potential and survival rate were obtained by intracellular recording. Membrane resistance and capacitance were measured by whole-cell patch clamp. Phosphatidyl serine and nucleic acid were double stained and simultaneously measured by annexin V and propidium iodide.
Results Lidocaine at a clinical dose (5–20 mM) induced morphological change (bulla and bleb) in the neuron and increased cell size in a concentration-dependent manner. Membrane potential was depolarized in a concentration-dependent manner. At perfusion of more than 5 mM lidocaine, the depolarized membrane potential was irreversible. Lidocaine decreased membrane resistance and increased membrane capacitance in a concentration-dependent manner. Both phosphatidyl serine and nucleic acid were stained under lidocaine exposure in a concentration-dependent manner.
Conclusions A clinical dose of lidocaine greater than 5 mM destroys the cell membrane and induces both necrosis and apoptosis in an identified *Lymnaea* neuron.

Keywords Lidocaine · Necrosis · Apoptosis · Annexin

Introduction

Lidocaine is commonly used for regional anesthesia and postoperative pain relief. However, neural injury after spinal anesthesia initially seems to result from the specific effects of lidocaine, because most reported cases of cauda equina syndrome have occurred in patients who have received spinal anesthesia using this agent [1–3]. Anesthesiologists have become concerned about irreversible neural injury caused by lidocaine. To clarify the mechanisms of such neurotoxicity, numerous studies have been performed in the fields of animal behavior, electrophysiology, and histopathology [4, 5]. We have also reported that lidocaine induced neurotoxicity with morphological changes such as cell axon collapse and cell swelling [6, 7]. It has been demonstrated that one of the mechanisms of neurotoxicity by lidocaine is apoptosis through the mitochondrial pathway [8, 9]. We have also reported that lidocaine induces apoptosis through the mitochondrial pathway by intracellular alkalization and increases in intracellular calcium and sodium [10–12]. In contrast, lidocaine-induced necrosis has also been reported [13, 14]. Increases in intracellular Ca^{2+}, Na^{+}, and pH can result in apoptosis or necrosis [15–17]. For example, dynamic

S. Onizuka (✉) · R. Tamura · T. Yonaha · N. Oda · Y. Kawasaki · T. Shirasaka · I. Tsuneyoshi
Department of Anesthesiology and Intensive Care, Faculty of Medicine, University of Miyazaki, Kiyotake-Cho, Miyazaki 889-1692, Japan
e-mail: pirotann@med.miyazaki-u.ac.jp

S. Shiraishi
Innovative Pathophysiology Research Group, Division of Cancer Pathophysiology, National Cancer Center Research Institute, 5-1-1 Tsukiji, Chuo-ku, Tokyo 104-0045, Japan

membrane blebbing is caused by the increased contractility of the acto-myosin system following myosin light chain (MLC) phosphorylation. MLC phosphorylation is a consequence of the cleavage of a Rho GTPase effector, the kinase ROCK I, by caspase-3 activation, and this caspase-3 activation is brought about by these intracellular Ca^{2+}, Na^{+}, and pH increases [18–20]. However, different kinds of evidence and many mechanisms for lidocaine-induced apoptosis and necrosis have been presented. Commonly, in necrosis, cell size is increased and cell swelling occurs, whereas cell size is decreased in apoptosis [21, 22]. We speculate that irreversible nerve injury results from the direct destruction of the cell membrane by lidocaine. To demonstrate this hypothesis, morphological changes such as cell size, survival rate, membrane potential, membrane resistance, cell capacitance, and induction of apoptosis or necrosis by lidocaine were examined.

Materials and methods

Animal and cell culture

All animal experiments were approved by the Animal Care Committee of the University of Miyazaki. Specifically, individually identified left pedal dorsal 1 (LPeD1) neurons from laboratory-raised *Lymnaea stagnalis* (freshwater snail) were used at room temperature. The snails were deshelled and transferred to a sterile dissection dish in normal *Lymnaea* saline [51.3 mM NaCl, 1.7 mM KCl, 4.1 mM $CaCl_2$, 1.5 mM $MgCl_2$, and 5.0 mM *N*-2-hydroxyethylpiperazine-*N*-2-ethanesulfonic acid (HEPES), pH 8, with NaOH]. The ganglia were treated in a defined medium [serum-free 50% Leibovitz L-15 medium (GIBCO-BRL Life Technologies, Burlington, Ontario, Canada) with added inorganic salts, 20 μg/ml gentamycin, pH 7.9] for 25 min with 0.2% trypsin (type III; Sigma Chemical, St. Louis, MO, USA). The neurons were removed by gentle suction with a siliconized, microforge fine-polished pipette with outside diameter of 1.5 mm (IB-150 F; WPI, Sarasota, FL, USA). The neurons then were transferred to poly-L-lysine-coated culture dishes (Falcon Plastics, Los Angeles, CA, USA) with 3 ml of the defined medium [23].

Measurement of cell size

For comparison, the cell sizes were measured before and after 10 min lidocaine perfusion. Cells were photographed using a Sony XC-003 3CCD digital camera attached to a microscope (Nikon TE-300). Sample cells from the digital images were analyzed on a PC computer using the public domain image analysis program developed at the U.S. National Institutes of Health (NIH Image; Scion, Frederick, MD, USA). The recorded images were saved in a Scion-compatible TIFF format and then imported into the program. Calibration was performed for each image by drawing a line over the scale that was introduced into the image field before digitization [24]. With the line tool, the areas of the sample cells were automatically drawn and measured. The output of the measured areas was transferred to an Excel program to calculate mean areas.

Intracellular recording

Neuronal activity was monitored using conventional intracellular recording [25]. A glass microelectrode with a filament and an outside diameter of 1.5 mm (TW150F-4; WPI) was filled with a KCl pipette solution consisting of 50 mM KCl, 10 mM HEPES, and 2 mM ATP-Mg. The pH was clamped to 7.0 with KOH, yielding a tip resistance of 20–30 MΩ. Electrical signals were amplified with a current–voltage clamp amplifier (Multiclamp-700A; Axon Instruments, Union City, CA, USA). For control and data acquisition, an AD and DA converter (Digidata 1322A; Axon Instruments) was used. Data acquisition and analysis were conducted using pClamp 9 software (Axon Instruments). Lidocaine was perfused for 10 min at each concentration. Live LPeD1 cells have membrane potential less than −50 mV and induce depolarization by current stimulation; however, in contrast, apoptotic or necrotic cells lose their membrane potential and do not depolarize by current stimulation. Therefore, after 60-min washout, the survival rate, defined as "survive," was calculated through observation by recovery of the membrane potential to less than −50 mV and depolarization by 0.5-nA current injection.

Membrane resistance measurement by patch-clamp recordings

Whole-cell patch-clamp recordings in the *Lymnaea* neuron were made using a multiclamp 700 A amplifier (Axon Instruments) [26, 27]. Patch electrodes (tip diameter adjusted to 1.0 μm; resistance, 1–3 MΩ) were pulled from glass tubing (outside diameter, 1.5 mm) with no filament (PG-150T-7.5; Warner Instrument, Hamden, CT, USA) on a vertical pipette puller (PA-10; Narishige, Tokyo, Japan). For control and data acquisition, an AD and DA converter interface board (Digidata 1322A; Axon Instruments) was inserted into a personal computer. Data acquisition and analysis were conducted using pClamp 9 software (Axon Instruments). The current was filtered at 1 kHz using a 4-pole Bessel filter and digitized at a sampling frequency of 20 kHz. To study membrane resistance and capacitance, pipettes were filled with a standard potassium pipette solution consisting of 50 mM KCl, 5 mM ethylene glycol tetraacetic acid (EGTA), 10 mM HEPES, and 2 mM

ATP-Mg; pH was adjusted to 7.4 (with KOH). For whole-cell patch clamp, after obtaining a gigaohm seal, the membrane was ruptured by suction with a syringe, and then the membrane resistance and membrane capacitance were continuously recorded. All experiments were performed at room temperature (20–22°C).

Double staining with propidium iodide and annexin V

An analysis of phosphatidyl serine on the outer leaflet of apoptotic cell membranes was performed using annexin V-FITC to identify apoptotic cells. Necrotic cells were identified by propidium iodide [28]. Each sample cell was incubated with 1 ml staining solution with 10 μM annexin V-FITC and 10 μM propidium iodide in normal saline for 15 min. Evaluation was by fluorescence microscopy using 488 nm excitation and emission at 505 nm for annexin V-FITC and at 590 nm for propidium iodide.

Experimental procedure

In each trial, lidocaine (1, 5, 10, 15, or 20 mM) was perfused into the culture dish for 10 min after the baseline values were measured.

Statistical analysis

The results are expressed as the mean ± standard deviation (SD). Plots were fitted to a Hill equation of the form $y = \text{base} + (\text{max–base})/[1 + (\text{Xhalf/X})^{\text{rate}}]$, where the rate is the Hill coefficient and Xhalf is the half-maximal response (EC_{50}), calculated using Igor Pro software (Version 5.01; WaveMetrics, Tigard, OR, USA).

The results of repeated measurements at each dose for each group of trials were analyzed by repeated-measures one-way analysis of variance (ANOVA), followed by Scheffe's test. StatView (version 4.5; Abacus, Canoga Park, CA, USA) was used for these analyses. $P < 0.05$ was considered to be statistically significant.

Results

Morphological changes by lidocaine

Figure 1a presents photographs of an LPeD1 neuron before and after administration of each concentration of lidocaine. Lidocaine concentration-dependently increased the cell size with E_{max} of 137% ± 11% at 20 mM and EC_{50} 8.6 mM.

Swelling and blebbing were induced in each neuron in a concentration-dependent manner (Fig. 1a,b).

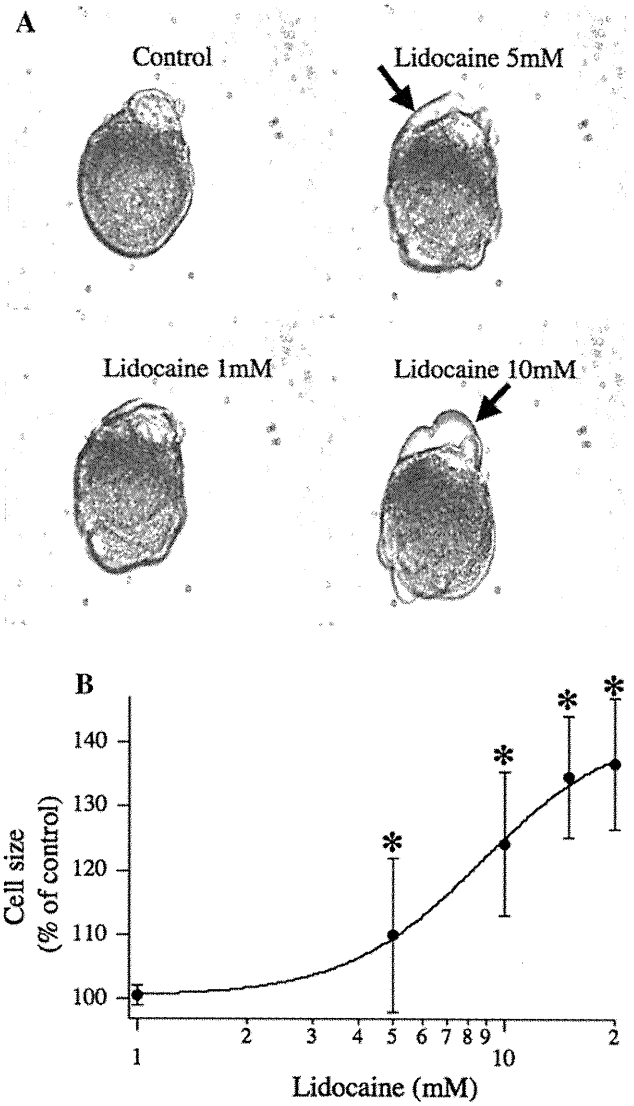

Fig. 1 **a** Morphological changes before and after lidocaine perfusion for 10 min at each concentration. **b** Areas of the sample cells were measured and analyzed by using NIH imaging. Results are presented as mean ± SD, $n = 5$. *$P < 0.05$ in comparison to control values

Irreversible depolarization by lidocaine

Lidocaine induced membrane depolarization in a concentration-dependent manner to −62 ± 11 mV at control, −52 ± 8 at 1 mM, −35 ± 8 at 5 mM, −8 ± 8 at 10 mM, −8 ± 8 at 10 mM, 1.4 ± 3 at 15 mM, and 2.5 ± 3 at 20 mM, with a half-maximal response at 6.2 mM (Fig. 2b). Depolarization at more than 5 mM lidocaine was irreversible after washout for 60 min. In contrast, with 1 mM lidocaine perfusion for 10 min, membrane depolarization recovered after washout (Fig. 2a). Figure 2c shows survival rates 60 min after washout. The effective dose for 50% fatality (ED_{50}) was 7.5 mM.